

Dynamics of heavy flavor in a weakly magnetized hot QCD medium

Debarshi Dey^{*} and Binoy Krishna Patra[†]

Department of Physics, Indian Institute of Technology Roorkee, Roorkee 247667, India

 (Received 4 September 2023; revised 22 January 2024; accepted 14 May 2024; published 10 June 2024)

We obtain the spatial and momentum-diffusion coefficients (D_s and κ) and the collisional energy loss (dE/dx) of a heavy quark (HQ) traversing through a thermal medium of quarks and gluons in a weak magnetic field (B), for the two cases of the HQ moving either parallel or perpendicular to B . For that purpose, we consider Coulomb scatterings (t -channel) of the HQ with the light quarks, obtained from the imaginary part of the HQ self-energy via the cutting rules. Both the normalized (by T^3) κ , and dE/dx , for charm quarks are larger than that for bottom quarks due to the larger mass of the latter. Also, the effect of B is more feeble on the bottom quark, compared to the charm quark. Comparatively, the magnitudes of both κ and dE/dx are significantly smaller for the case of $\mathbf{v} \perp \mathbf{B}$. For both the cases, our results show that the momentum transfer between the HQ and the medium takes place preferentially along the direction of HQ velocity, thus leading to a significant increase in the momentum-diffusion anisotropy, compared to $B = 0$. We also calculate the (scaled) spatial diffusion coefficient, which we find to be independent of the heavy flavor mass and is almost unaffected by changes in B .

DOI: [10.1103/PhysRevD.109.116008](https://doi.org/10.1103/PhysRevD.109.116008)

I. INTRODUCTION

Heavy-ion collisions at experimental facilities such as the Relativistic Heavy Ion Collider (RHIC) and the Large Hadron Collider have presented strong evidence of formation of a deconfined thermal QCD medium, called the quark gluon plasma (QGP) [1,2]. When the heavy nuclei collide noncentrally, the spatial asymmetry of the initial overlap zone is carried over to the momenta of emitted particles and can be seen experimentally in the final hadron p_T spectra [3–6]. This asymmetric expansion of the QGP fireball is referred to as elliptic flow. A remarkable property of this medium is the very small value of the ratio of shear viscosity to entropy density η/s , making QGP one of the most perfect fluids known [7]. A microscopic explanation of these interesting transport properties is still a subject of intense investigation. To that end, heavy quarks (charm and bottom) are considered to be excellent probes of the QGP medium [8]. The large mass of the heavy quark M_Q compared to the temperature of the medium ($M_Q \gg T$) means that heavy quarks are formed at very early stages of heavy-ion collisions, even before the formation of the thermal medium [9]. Typical heavy quark (HQ) formation

time is $\sim 1/2M_Q$ [10] (~ 0.08 fm/c for charm and ~ 0.03 fm/c for bottom). Furthermore, compared to the light quarks, the HQ thermal relaxation times are larger, parametrically by a factor $M_Q/T \sim 5$ –15. The light quark and gluon thermalization time $\tau_{q,g}$ is ~ 0.6 fm, as indicated by hydrodynamic modeling of the RHIC data [11]. This implies a HQ thermalization time of 3–9 fm/c, which is of the order of (for charm) or larger than (for bottom) the estimated QGP lifetime of ~ 5 fm/c [12]. Because of being created so early and not equilibrating fully with the medium, the HQs are witnesses to the full history of space-time evolution of the medium and also retain a “memory” of their interactions with the medium. This makes heavy quarks ideal probes of the QGP medium. Extensive discussions on HQ phenomenology can be found in Refs. [12,13].

Apart from causing an anisotropic expansion of the created matter, noncentral heavy-ion collisions also lead to creation of large magnetic fields [14]. The decay rate of the magnetic field depends strongly on the electrical conductivity of the medium which is exposed to the field [15–24]. Assuming a large background magnetic field, several phenomena have been studied such as chiral magnetic effect [25], chiral magnetic wave [26,27], charge-dependent elliptic flow [28,29], magnetic catalysis [30–32], inverse magnetic catalysis [33–39], etc. For small conductivities, however, the magnetic field decay would be very fast. This has led to studies of QGP transport properties in a weak background magnetic field in the recent past [24,40–49]. For the case of HQs, their production times are small ($\sim 1/2M_Q$). This is similar to the

^{*}ddey@ph.iitr.ac.in, debs.mvm@gmail.com

[†]binoy@ph.iitr.ac.in

Published by the American Physical Society under the terms of the Creative Commons Attribution 4.0 International license. Further distribution of this work must maintain attribution to the author(s) and the published article's title, journal citation, and DOI. Funded by SCOAP³.

timescale of generation of a (strong) magnetic field. However, in the plasma frame, the heavy quarks are formed at a time $t_f (= \gamma \tau_f)$ which could be of the order of 1–2 fm, depending on the momenta of the produced HQ. By that time, the strength of the magnetic field may become weak. Furthermore, although HQ transport has been studied in the presence of a strong background magnetic field, using both imaginary and real time formalism [50–53], the literature using a weak background magnetic field is rather scant. This motivates us to investigate the dynamics of individual heavy flavor in the QGP medium, in the limit of a weak background magnetic field. In the context of heavy quarks, the diffusion of HQ in a thermal medium has been studied using perturbation theory [54–65], lattice QCD [66–69], and in a Polyakov-loop plasma [70]. HQ dynamics in the presence of external EM fields has been studied in [10,71], where, in the former, the authors show that the directed flow (v_1) of HQs is a good probe of the magnetic field generated in noncentral heavy-ion collisions. In the latter study, the combined effect of the initial tilt of the QGP fireball and large EM fields on the HQ v_1 is studied. Effects of the initial preequilibrium glasma phase on HQ observables have been explored in [72,73]. HQ drag and diffusion in strongly coupled plasmas have been studied in [74,75]. Next-to-leading-order calculation of the HQ diffusion has also been carried out [76]. The effect of momentum anisotropy on the dynamics of HQ has also been studied recently [77,78]. Recently, a nonperturbative study of HQ diffusion in strong magnetic fields has been carried out [79].

The HQ mass is the hardest scale in the problem, which is true even if the magnetic field is strong. The scale hierarchy considered in this problem is $M_Q \gg T \gg eB/T$. We calculate the energy loss dE/dx and momentum-diffusion coefficients κ of the HQ moving with a finite velocity in the QGP by evaluating the scattering rate of the HQ with the light thermal quarks and gluons. In particular, we consider two cases of the HQ velocity: one in which the HQ velocity is parallel to \mathbf{B} and the other in which the HQ velocity lies in a plane perpendicular to \mathbf{B} . Cutting rules allow for determination of this scattering rate from the imaginary part of the HQ self-energy [80]. This method was employed to study HQ dynamics for the first time in [55]. In what follows, the HQ self-energy is evaluated using an effective gluon propagator, which, in turn, is calculated in the presence of a weak magnetic field, up to second order in qB . Hard Thermal Loop (HTL) perturbation theory is made use of throughout the calculations. Owing to its large mass, the problem of HQ immersed in a thermal bath of light particles is amenable to a nonrelativistic treatment, in general, and a diffusion treatment, in particular, as will be justified in the next section. We go beyond the static heavy quarks and evaluate the aforementioned quantities for finite HQ momentum.

The paper is organized as follows: In Sec. II, the description of heavy quarks in a thermal medium is presented, wherein the case of zero magnetic field is discussed first, followed by the case of a finite magnetic field. Then, in Sec. III, the calculation of the scattering rate Γ in the presence of a weak magnetic field is outlined. In Sec. IV, the evaluation of energy loss dE/dx and momentum-diffusion coefficients κ are presented, first for the case $\mathbf{v} \parallel \mathbf{B}$, followed by the case $\mathbf{v} \perp \mathbf{B}$. In Sec. V, the results obtained are discussed. In Sec. VI, phenomenological applications of the calculations are described. Finally, we conclude in Sec. VII.

II. DESCRIPTION OF HEAVY QUARKS IN A THERMAL MEDIUM: STATIC CASE AND BEYOND

A. Kinematics in the absence of magnetic field

We consider a heavy quark of mass M_Q propagating through a plasma of light quarks and gluons. The HQ thermal momentum $p \sim \sqrt{M_Q T} \gg T$ translates to a thermal velocity $v \sim \sqrt{T/M_Q} \ll 1$. Even if one considers hard scatterings of the HQ with the light medium particles [characterized by a momentum transfer of $\mathcal{O}(T)$], it takes a large number of collisions ($\sim M_Q/T$) to change the HQ momentum by $\mathcal{O}(1)$, since $p \gg T$. This implies that the momentum changes accumulate over time from uncorrelated “kicks,” and the HQ momentum, therefore, evolves according to Langevin dynamics:

$$\frac{dp_i}{dt} = \xi_i(t) - \eta_D p_i, \quad \langle \xi_i(t) \xi_j(t') \rangle = \kappa \delta_{ij} \delta(t - t'), \quad (1)$$

where $(i, j) = (x, y, z)$. These are the macroscopic Langevin equations with η_D being the momentum drag coefficient and κ the momentum-diffusion coefficient. The random forces $\xi(t)$ representing the uncorrelated momentum kicks are assumed to be white noises. The solution of Eq. (1) under the assumption $\eta_D^{-1} \ll t$ is given as

$$p_i(t) = \int_{-\infty}^t dt' e^{\eta_D(t-t')} \xi_i(t'). \quad (2)$$

κ can be determined by calculating the mean squared momentum transfer per unit time from the underlying microscopic theory:

$$\langle p^2 \rangle = \int dt_1 dt_2 e^{\eta_D(t_1+t_2)} \langle \xi_i(t_1) \xi_j(t_2) \rangle = \frac{3\kappa}{2\eta_D}. \quad (3)$$

Equivalently, κ can be defined as

$$3\kappa(\mathbf{p}) = \lim_{\Delta t \rightarrow 0} \frac{\langle (\Delta p)^2 \rangle}{\Delta t}, \quad (4)$$

where, $\Delta p = p(t + \Delta t) - p(t)$. This leads to the following equations of motion for the heavy quark:

$$\frac{d}{dt} \langle p \rangle \equiv -\eta_D \langle p \rangle, \quad (5)$$

$$\frac{1}{3} \frac{d}{dt} \langle (\Delta p)^2 \rangle \equiv \kappa(p). \quad (6)$$

The drag coefficient or the relaxation rate η_D is related to κ via the fluctuation-dissipation relation

$$\eta_D = \frac{\kappa}{2M_Q T}, \quad (7)$$

which follows from general thermodynamical arguments. Apart from η_D and κ , we also have the spatial diffusion coefficient D_s and the heavy quark energy loss dE/dx . The problem of HQ motion and its subsequent diffusion in a thermal medium can be characterized fully by these four quantities, which are related to each other. In particular,

$$D_s = \frac{T}{M_Q \eta_D} = 2T^2/\kappa, \quad (8)$$

as derived in [81]. In a thermal medium of light quarks and gluons, the random momentum kicks originate from the scattering processes $qH \rightarrow qH$ and $gH \rightarrow gH$ ($q \rightarrow$ quark and $g \rightarrow$ gluon). The former occurs only via t -channel Coulomb scattering. The latter effectively also occurs via the same mechanism, since its Compton amplitude is suppressed by $v^2 \sim T/M_Q$, in the rest frame of the plasma. This is especially true for the bottom quark ($M = 4.18$ GeV), compared to the charm quark ($M = 1.28$ GeV). We assume that the dominant mechanism for the HQ energy loss is Coulomb scattering of the HQ with the light medium particles and ignore radiative energy loss (gluon bremsstrahlung), which is suppressed by an additional power in the strong coupling α_s , as explained in [56]. The central quantity from which all the above-mentioned dynamical quantities can be obtained is the scattering rate Γ , whose computation will be outlined in the next section. The energy loss and the momentum-diffusion coefficient are given, respectively, as

$$\frac{dE}{dx} = \frac{1}{v} \int d^3q \frac{d\Gamma(q)}{d^3q} q_0, \quad (9)$$

$$3\kappa = \int d^3q \frac{d\Gamma(q)}{d^3q} q^2. \quad (10)$$

$\frac{d\Gamma(q)}{d^3q}$ is the differential probability per unit time for the heavy quark momentum to change by \mathbf{q} . It can also be interpreted as the scattering rate of heavy quark via one-gluon exchange with thermal partons per unit volume of momentum transfer \mathbf{q} . v is the heavy quark velocity. q_0 and q are respectively the

energy and 3-momentum (magnitude) of the exchanged gluon. The factor of 3 comes from assuming isotropicity of the momentum-diffusion coefficient, which is valid if the heavy quark under consideration is assumed to be static and the background magnetic field is weak.

Beyond the case of static heavy quarks, the motion of the HQ along a particular direction leads to the generalized Langevin equations:

$$\frac{dp_i}{dt} = \xi_i(t) - \eta_D p_i, \quad \langle \xi_i(t) \xi_j(t') \rangle = \kappa_{ij}(\mathbf{p}) \delta(t - t'), \quad (11)$$

where $\kappa_{ij}(\mathbf{p}) = \kappa_L(p) \hat{p}_i \hat{p}_j + \kappa_T(p) (\delta_{ij} - \hat{p}_i \hat{p}_j)$. κ_L and κ_T are the longitudinal and transverse momentum-diffusion coefficients, respectively. The direction of HQ velocity defines an anisotropy direction, and the momentum-diffusion coefficient breaks into longitudinal and transverse components as $3\kappa \rightarrow \kappa_L + 2\kappa_T$. The factor of 2 reflects the fact that there are two equivalent transverse directions:

$$\kappa_L = \int d^3q \frac{d\Gamma(q)}{d^3q} q_L^2, \quad (12)$$

$$\kappa_T = \frac{1}{2} \int d^3q \frac{d\Gamma(q)}{d^3q} q_T^2. \quad (13)$$

The HQ momentum can be diffused via collisions, in the direction of HQ momentum and also transverse to it, of which, κ_L and κ_T , respectively, are quantitative measures. κ_L and κ_T will separately satisfy Einstein relations as follows:

$$(\eta_D)_L = \frac{\kappa_L}{2M_Q T}, \quad (\eta_D)_T = \frac{\kappa_T}{2M_Q T}. \quad (14)$$

B. Kinematics with a finite magnetic field

The presence of a magnetic field introduces an additional scale in the system. In this work, the strength of the magnetic field is considered to be weak; that is, the scale hierarchy satisfies $M_Q \gg T \gg eB/T$. The direction of the external magnetic field causes an anisotropy in the momentum-diffusion coefficients, similar to what was discussed earlier. Considering the case of static HQ and taking the direction of the external magnetic field to be along \hat{z} direction, one obtains the following Langevin equations corresponding to directions parallel and perpendicular to the magnetic field [50]:

$$\frac{dp_z}{dt} = -(\eta_D)_\parallel p_z + \xi_z, \quad \langle \xi_z(t) \xi_z(t') \rangle = \kappa_\parallel(\mathbf{p}) \delta(t - t'), \quad (15)$$

$$\frac{d\mathbf{p}_\perp}{dt} = -(\eta_D)_\perp \mathbf{p}_\perp + \boldsymbol{\xi}_\perp, \quad \langle \boldsymbol{\xi}_\perp(t) \boldsymbol{\xi}_\perp(t') \rangle = \kappa_\perp(\mathbf{p}) \delta(t - t'), \quad (16)$$

where η_z and $\boldsymbol{\eta}_\perp$ are the components of random forces parallel and perpendicular to \mathbf{B} , respectively, and the momentum-diffusion coefficients are obtained as

$$\kappa_\parallel = \int d^3q \frac{d\Gamma(E)}{d^3q} q_\parallel^2, \quad (17)$$

$$\kappa_\perp = \frac{1}{2} \int d^3q \frac{d\Gamma(E)}{d^3q} \mathbf{q}_\perp^2. \quad (18)$$

The longitudinal and transverse drag and diffusion coefficients separately satisfy fluctuation-dissipation relations, as earlier:

$$(\eta_D)_\parallel = \frac{\kappa_\parallel}{2M_Q T}, \quad (\eta_D)_\perp = \frac{\kappa_\perp}{2M_Q T}. \quad (19)$$

Now, if the HQ also has a velocity along a certain direction, then one needs to consider the interplay between the directions of HQ velocity and magnetic field.

1. Case 1: $\mathbf{v} \parallel \mathbf{B}$

In the first case, we consider the HQ velocity to be along the direction of the magnetic field, so that, effectively, we still have a single preferred direction in space (\hat{z}). Then, one obtains the longitudinal and transverse momentum-diffusion coefficients, respectively, as

$$\kappa_L = \int d^3q \frac{d\Gamma(E, v)}{d^3q} q_z^2, \quad (20)$$

$$\kappa_\perp = \frac{1}{2} \int d^3q \frac{d\Gamma(E, v)}{d^3q} \mathbf{q}_\perp^2. \quad (21)$$

2. Case 2: $\mathbf{v} \perp \mathbf{B}$

The HQ velocity could also be in a plane perpendicular to \mathbf{B} (i.e., the x - y plane). In such a case, one generally defines three momentum-diffusion coefficients based on the direction of momentum transfer, as

$$\kappa_1 = \int d^3q \frac{d\Gamma(E, v)}{d^3q} q_x^2, \quad (22)$$

$$\kappa_2 = \int d^3q \frac{d\Gamma(E, v)}{d^3q} q_y^2, \quad (23)$$

$$\kappa_3 = \int d^3q \frac{d\Gamma(E, v)}{d^3q} q_z^2. \quad (24)$$

As we shall see, the structure of integrations will be different for the two cases.

III. PERTURBATIVE DETERMINATION OF SCATTERING RATE Γ

As mentioned earlier, we consider Coulomb scattering of the propagating heavy quark with the thermal quarks and gluons. To leading order, these $2 \rightarrow 2$ processes are represented by the following tree-level Feynman diagrams. The double line represents the heavy quark, whereas the thermal light quark is represented by the single line. Γ calculated using the tree-level diagrams in Fig. 1 turns out to be quadratically infrared divergent, which corroborates with the well-known fact that the total rate of Coulomb scattering in a plasma is quadratically infrared divergent [82]. Using a resummed gluon propagator in Fig. 1 instead of a bare one softens the divergence to a logarithmic one [55]. This arises because the dynamical screening of the magnetic interaction provided by the transverse effective propagator is not sufficient to completely screen the divergence from the long-range static magnetic interaction. However, the two additional powers of q in Eq. (10) render κ infrared finite. The presence of the logarithm reflects that Γ receives contribution from both the soft and hard momentum transfers. Soft processes involve $\mathbf{q} \sim gT$ and occur at a rate $\Gamma_{\text{soft}} \sim g^2 T$, whereas the relatively scarce hard processes correspond to $\mathbf{q} \sim T$ and occur at a rate $\Gamma_{\text{hard}} \sim g^4 T$. In this article, we shall be evaluating the soft contribution to Γ and, therefore, to the heavy quark diffusion coefficient, since it dominates over hard processes.

An efficient method of calculating the scattering rate was put forward by Weldon [80], wherein Γ is evaluated from the imaginary part of the heavy quark self-energy:

$$\begin{aligned} \Gamma(P \equiv E, \mathbf{v}) &= -\frac{1}{2E} [1 - n_F(E)] \text{Tr}[(\boldsymbol{P} + M_Q) \text{Im}\Sigma(p_0 + i\epsilon, \mathbf{p})]. \end{aligned} \quad (25)$$

The imaginary part of the heavy quark self-energy is related to the squared amplitude for Coulomb scattering processes via the cutting rules, for the two-loop self-energy diagrams shown in Fig. 2. This procedure automatically rules out using one-loop self-energy diagrams, since the cut (imaginary) parts of those diagrams correspond to processes which do not conserve energy-momentum and, thus, are unphysical [83]. The hard contribution to Γ comes from the two-loop self-energy diagrams in Fig. 2. However, when

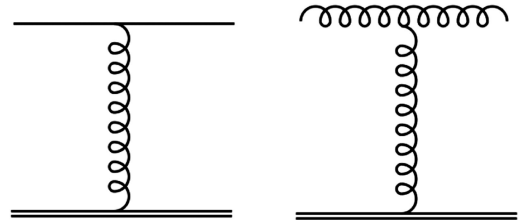


FIG. 1. Feynman diagrams of processes contributing to heavy quark diffusion at leading order.

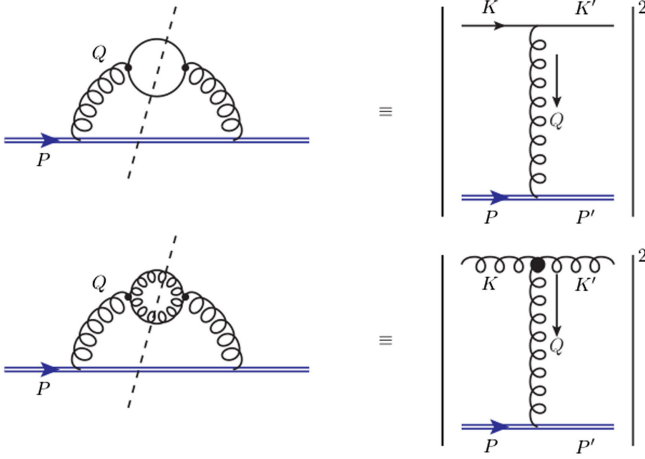


FIG. 2. Cut (imaginary) part of heavy quark self-energy diagrams yields the amplitude squared of t channel scattering processes $qH \rightarrow qH$ and $gH \rightarrow gH$.

the gluon momentum is soft, hard thermal loop corrections to the gluon propagator contribute at leading order in the strong coupling g and, therefore, must be resummed. The resummed propagator is obtained by summing all possible self-energy corrections proportional to $g^2 T^2$ to the bare propagator, as shown in Fig. 3. This is a geometric series summation, where the second and third diagrams are nominally of the order of $g^2 T^2$. Similarly, the fourth and fifth diagrams are $\mathcal{O}(g^4 T^4)$, and so on [55]. The self-energy diagram, therefore, to be evaluated is the heavy quark self-energy with resummed gluon propagator (Fig. 4). We use the imaginary time formalism to compute the heavy quark self-energy $\Sigma(P)$. Using Feynman rules, $\Sigma(P)$ in a weak background magnetic field is given by

$$\Sigma(P) = ig^2 \int \frac{d^4 Q}{(2\pi)^4} \mathcal{D}^{\mu\nu}(Q) \gamma_\mu S(P-Q) \gamma_\nu. \quad (26)$$

Since we work in the regime $\frac{qB}{M_Q} \ll 1$, we can ignore Landau quantization of the heavy quark energy levels,

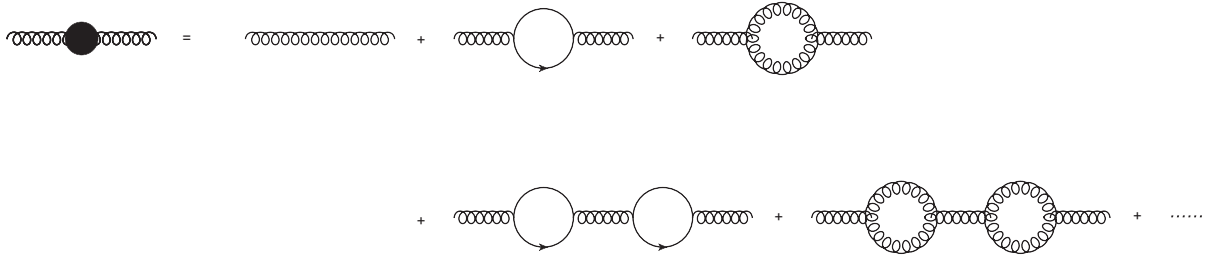


FIG. 3. Resummed gluon propagator. In addition to the leading-order diagrams, resummation takes into account all higher-order diagrams that contribute to leading order in g .

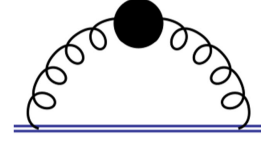


FIG. 4. HQ self-energy diagram with resummed gluon propagator.

as has been done in [51], and write the heavy quark propagator as

$$iS(P-Q \equiv K) = i \frac{\not{K} + M_Q}{K^2 - M_Q^2}. \quad (27)$$

The effective gluon propagator in the presence of a weak magnetic field is expressed as [84]

$$\begin{aligned} \mathcal{D}^{\mu\nu}(Q) = & \frac{\xi Q^\mu Q^\nu}{Q^4} + \frac{(Q^2 - d)\Delta_1^{\mu\nu}}{(Q^2 - b)(Q^2 - d) - a^2} + \frac{\Delta_2^{\mu\nu}}{Q^2 - c} \\ & + \frac{(Q^2 - b)\Delta_3^{\mu\nu}}{(Q^2 - b)(Q^2 - d) - a^2} \\ & + \frac{a\Delta_4^{\mu\nu}}{(Q^2 - b)(Q^2 - d) - a^2}, \end{aligned} \quad (28)$$

where

$$b(Q) = \Delta_1^{\mu\nu} \Pi_{\mu\nu}, \quad (29a)$$

$$c(Q) = \Delta_2^{\mu\nu} \Pi_{\mu\nu}, \quad (29b)$$

$$d(Q) = \Delta_3^{\mu\nu} \Pi_{\mu\nu}, \quad (29c)$$

$$a(Q) = \frac{1}{2} \Delta_4^{\mu\nu} \Pi_{\mu\nu}. \quad (29d)$$

$\Pi_{\mu\nu}(Q)$ is the gluon self-energy computed within the HTL approximation. $\Delta_i^{\mu\nu}$ are the projection tensors along which the gluon self-energy and the effective gluon propagator are expressed in the presence of a finite magnetic field,

details of which can be found in Appendix A. They are expressed as

$$\Delta_1^{\mu\nu} = \frac{1}{\bar{u}^2} \bar{u}^\mu \bar{u}^\nu, \quad (30a)$$

$$\Delta_2^{\mu\nu} = g_{\perp}^{\mu\nu} - \frac{Q_{\perp}^\mu Q_{\perp}^\nu}{Q_{\perp}^2}, \quad (30b)$$

$$\Delta_3^{\mu\nu} = \frac{\bar{n}^\mu \bar{n}^\nu}{\bar{n}^2}, \quad (30c)$$

$$\Delta_4^{\mu\nu} = \frac{\bar{u}^\mu \bar{n}^\nu + \bar{u}^\nu \bar{n}^\mu}{\sqrt{\bar{u}^2} \sqrt{\bar{n}^2}}. \quad (30d)$$

u^μ is the velocity of the heat bath, and n^μ can be considered to define the direction of the background magnetic field. Evaluating the form factors $b(Q)$, $c(Q)$, $d(Q)$, and $a(Q)$ of Eq. (29) is akin to evaluating the effective gluon propagator. The calculation of these form factors under HTL approximation, along with the other tensors in Eq. (30), is detailed in Appendix B.

Following [52], we next evaluate the trace in Eq. (25):

$$\begin{aligned} & \text{Tr}[(\not{P} + M_Q)\Sigma(P)] \\ &= ig^2 \int \frac{d^4 Q}{(2\pi)^4} \frac{1}{K^2 - M_Q^2} \\ & \times \sum_{i=1}^4 \chi_i \text{Tr}[(\not{P} + M_Q)\Delta_i^{\mu\nu} \gamma_\mu (K + M_Q)\gamma_\nu]. \quad (31) \end{aligned}$$

$$\text{Tr}[(\not{P} + M_Q)\Delta_1^{\mu\nu} \gamma_\mu (K + M_Q)\gamma_\nu] = \frac{4}{\bar{u}^2} [2(P \cdot \bar{u})(K \cdot \bar{u}) + \bar{u}^2(M^2 - P \cdot K)] = A_1 + B_1, \quad (33a)$$

$$\text{Tr}[(\not{P} + M_Q)\Delta_2^{\mu\nu} \gamma_\mu (K + M_Q)\gamma_\nu] = 4 \left[2(P \cdot K)_\perp - \frac{2(P \cdot Q)_\perp (K \cdot Q)_\perp}{Q_{\perp}^2} + (M^2 - P \cdot K) \right] = A_2 + B_2, \quad (33b)$$

$$\text{Tr}[(\not{P} + M_Q)\Delta_3^{\mu\nu} \gamma_\mu (K + M_Q)\gamma_\nu] = \frac{4}{\bar{n}^2} [2(P \cdot \bar{n})(K \cdot \bar{n}) + \bar{n}^2(M^2 - P \cdot K)] = A_3 + B_3, \quad (33c)$$

$$\text{Tr}[(\not{P} + M_Q)\Delta_4^{\mu\nu} \gamma_\mu (K + M_Q)\gamma_\nu] = \frac{8}{\sqrt{\bar{n}^2} \sqrt{\bar{u}^2}} [(P \cdot \bar{u})(K \cdot \bar{n}) + (P \cdot \bar{n})(K \cdot \bar{u}) + (\bar{u} \cdot \bar{n})(M^2 - P \cdot K)] = A_4 + B_4. \quad (33d)$$

The traces have been separated into q_0 -independent and q_0 -dependent terms denoted by A_i and B_i , respectively; $i = 1, 2, 3, 4$. This is done to facilitate the frequency sum over q_0 , as will be seen later. The condition required for

Taking the gauge parameter ξ in Eq. (28) to be 0, the coefficients χ_i 's are given by

$$\chi_1 = \frac{(Q^2 - d)}{(Q^2 - b)(Q^2 - d) - a^2}, \quad (32a)$$

$$\chi_2 = \frac{1}{(Q^2 - c)}, \quad (32b)$$

$$\chi_3 = \frac{(Q^2 - b)}{(Q^2 - b)(Q^2 - d) - a^2}, \quad (32c)$$

$$\chi_4 = \frac{a}{(Q^2 - b)(Q^2 - d) - a^2}. \quad (32d)$$

It should be noted that the gauge can be fixed only when the quantity being calculated is known to be gauge invariant. In our case, the scattering rate Γ is known to be gauge invariant in QED as well as in QCD, as described in [55]. In fact, the soft and hard contributions to Γ are separately gauge invariant and can be calculated in any suitable gauge. In our case, we set $\xi = 0$, which corresponds to the Landau gauge.

We evaluate the individual traces in Eq. (31):

such a separation to be executed is that the transfer momentum four-vector Q^μ be spacelike, which is indeed the case for t -channel scattering processes. The A_i 's and B_i 's come out to be

$$A_1 = 4(2p_0^2 - \mathbf{p} \cdot \mathbf{q}), \quad B_1 = -8p_0^2 \frac{q_0^2}{q^2} - 8 \frac{q_0^2 (P \cdot Q)^2}{Q^2 q^2} + 16p_0 q_0 \frac{P \cdot Q}{q^2}, \quad (34)$$

$$A_2 = 4 \left[2\{P_{\perp}^2 - (P \cdot Q)_{\perp}\} - \mathbf{p} \cdot \mathbf{q} + \frac{2(P \cdot Q)_{\perp} \{Q_{\perp}^2 - (P \cdot Q)_{\perp}\}}{Q_{\perp}^2} \right], \quad B_2 = 4p_0 q_0, \quad (35)$$

$$A_3 = \frac{8}{\bar{n}^2} \left[p_3^2 - \frac{2p_3q_3}{q^2} (\mathbf{p} \cdot \mathbf{q}) + \frac{q_3}{q^2} (\mathbf{p} \cdot \mathbf{q})^2 - \frac{\bar{n}^2}{2} (\mathbf{p} \cdot \mathbf{q}) \right], \quad B_3 = 4p_0q_0, \quad (36)$$

$$A_4 = \frac{16}{\sqrt{\bar{n}^2}} \left[-p_0p_3 + \frac{p_0p_3}{q^2} (\mathbf{p} \cdot \mathbf{q}) \right] = \frac{16p_0p_3}{\sqrt{\bar{n}^2}} \left[\frac{\mathbf{p} \cdot \mathbf{q}}{q^2} - 1 \right], \quad (37)$$

$$B_4 = \frac{16}{\sqrt{\bar{n}^2}} \left[\frac{p_3q_0^2p_0}{q^2} - \frac{p_3q_0}{q^2} (\mathbf{p} \cdot \mathbf{q}) - \frac{q_0^2q_3p_0}{Q^2q^2} (\mathbf{p} \cdot \mathbf{q}) + \frac{q_0q_3}{Q^2q^2} (\mathbf{p} \cdot \mathbf{q})^2 \right] \left\{ \left(-\frac{q_0^2}{q^2} \right) + \text{higher powers of } \frac{q_0^2}{q^2} \right\}. \quad (38)$$

Next, we perform the frequency sum over q_0 . To that end, a convenient method is to introduce spectral representations for the propagators [85]. The fermion propagator is spectrally represented as

$$\begin{aligned} & \frac{1}{K^2 - M_Q^2} \\ &= -\frac{1}{2E'} \int_0^\beta d\tau' e^{k_0\tau'} [(1 - n_F(E'))e^{-E'\tau'} - n_F(E')e^{E'\tau'}], \end{aligned} \quad (39)$$

where $E' = \sqrt{k^2 + M_Q^2}$ and $\beta = 1/T$. Similarly, pieces of the effective gluon propagator χ_i can be expressed as

$$\chi_i = - \int_0^\beta d\tau e^{q_0\tau} \int_{-\infty}^{\infty} d\omega \rho_i(\omega, q) [1 + n_B(\omega)] e^{-\omega\tau}. \quad (40)$$

ρ_i are the spectral functions associated with χ_i and are odd functions of ω . Each spectral function contains contributions from both spacelike and timelike frequencies and is expressed as

$$\rho_i(\omega, q) = \rho_i^{\text{pole}}(\omega, q) + \rho_i^{\text{cut}}(\omega, q), \quad (41)$$

with

$$\rho_i^{\text{pole}}(\omega, q) = \rho_i^{\text{res}} \delta(\omega - \omega_i(q)), \quad (42)$$

$$\rho_i^{\text{cut}}(\omega, q) = \rho_i^{\text{dis}} \theta(q^2 - \omega^2). \quad (43)$$

Thus, the spectral functions have delta function contributions at the timelike points (poles) $\omega = \omega_i(q)$, where $\omega_i(q)$ are the dispersion relations and ρ_i^{res} are the residues at those points. For spacelike frequencies $|\omega| < q$, ρ_i 's receive a discontinuous contribution from the imaginary part of the resummed propagator (Landau damping):

$$\rho_i^{\text{dis}}(\omega, q) = -\frac{1}{\pi} \text{Im}(\chi_i|_{q_0=\omega+ie}). \quad (44)$$

Since we work in the regime $|\omega| < q$, only the cut part in Eq. (41) contributes and is denoted simply as ρ hereafter. The calculation and final expressions of the ρ_i 's are given in Appendix C. The advantage of the spectral function representation is that it simplifies the evaluation of the frequency sums due to the appearance of delta functions in the integral, coming from

$$T \sum_{q_0} e^{q_0(\tau-\tau')} = \delta(\tau - \tau'), \quad (45a)$$

$$T \sum_{q_0} q_0 e^{q_0(\tau-\tau')} = \delta'(\tau - \tau'). \quad (45b)$$

Using this, Eq. (31) becomes

$$\begin{aligned} \text{Tr}[(\mathcal{P} + M)\Sigma(P)] &= -ig^2 \int \frac{d^4Q}{(2\pi)^4} \frac{1}{K^2 - M_Q^2} \sum_{i=1}^4 \chi_i [A_i + B_i] \\ &= -g^2 T \sum_{i=1}^4 \int \frac{d^3q}{(2\pi)^3} \int_{-\infty}^{+\infty} d\omega [1 + n_B(\omega)] \int_0^\beta d\tau' \int_0^\beta d\tau e^{p_0\tau'} e^{-\omega\tau} \\ &\quad \times \sum_{q_0} e^{q_0(\tau-\tau')} [A_i + B_i] \frac{\rho_i(\omega, q)}{2E'} [\{1 - n_F(E')\}e^{-E'\tau'} - n_F(E')e^{E'\tau'}] \\ &= -g^2 T \sum_{i=1}^4 \int \frac{d^3q}{(2\pi)^3} \int_{-\infty}^{+\infty} d\omega [1 + n_B(\omega)] (I_1 + I_2), \end{aligned} \quad (46)$$

where, using Eq. (45a),

$$I_1 = \int_0^\beta d\tau' \int_0^\beta d\tau e^{p_0\tau'} e^{-\omega\tau} A_i \delta(\tau - \tau') \frac{\rho_i(\omega, q)}{2E'} [\{1 - n_F(E')\} e^{-E'\tau'} - n_F(E') e^{E'\tau'}]. \quad (47)$$

We use the δ function to integrate over τ' to obtain

$$I_1 = \int_0^\beta d\tau e^{(p_0 - \omega)\tau} \frac{\rho_i(\omega, q)}{2E'} [\{1 - n_F(E')\} e^{-E'\tau} - n_F(E') e^{E'\tau}] A_i. \quad (48)$$

The τ integration ultimately yields

$$I_1 = - \sum_{j=\pm 1} \frac{j n_F(jE')}{p_0 - \omega + jE'} [e^{(p_0 - \omega + jE')\beta} - 1] A_i. \quad (49)$$

Since B_i is q_0 dependent, a sample term can be written as $B_i = q_0 C_i$. Then, using Eq. (45b) yields

$$\begin{aligned} I_2 &= \int_0^\beta d\tau' \int_0^\beta d\tau e^{p_0\tau'} e^{-\omega\tau} \sum_i C_i \delta'(\tau - \tau') \frac{\rho_i(\omega, q)}{2E'} [\{1 - n_F(E')\} e^{-E'\tau'} - n_F(E') e^{E'\tau'}] \\ &= - \int_0^\beta d\tau \frac{d}{d\tau} e^{(p_0 - \omega)\tau} [\{1 - n_F(E')\} e^{-E'\tau} - n_F(E') e^{E'\tau}] C_i \\ &= \sum_{j=\pm 1} j n_F(jE') [e^{(p_0 - \omega + jE')\beta} - 1] C_i. \end{aligned} \quad (50)$$

p_0 is discrete, since we are working in the imaginary time formalism. Specifically, $p_0 = i(2n + 1)\pi/\beta$. At these discrete energies, $e^{p_0\beta} = -1$, and p_0 thus gets eliminated from the exponent in Eqs. (49) and (50). Thereafter, we analytically continue p_0 to real values via $p_0 \rightarrow E + i\omega$. The imaginary part is then extracted, which comes from energy denominator terms of the form

$$\text{Im} \left(\frac{1}{p_0 + E' - \omega} \right) \Big|_{p_0 \rightarrow E + i\omega} = -i\pi \delta(p_0 + E' - \omega). \quad (51)$$

Since there is no energy denominator in Eq. (50), I_2 does not have any imaginary part, and the contribution to the imaginary part of the self-energy thus comes solely from I_1 . Using Eqs. (46), (49), and (51), we can write

$$\begin{aligned} \text{Tr}[(\boldsymbol{P} + M_Q) \text{Im}\Sigma(p_0 + i\epsilon, \boldsymbol{p})] &= \pi g^2 \sum_{i=1}^4 \int \frac{d^3 q}{(2\pi)^3} \int_{-\infty}^{\infty} d\omega [1 + n_B(\omega)] \frac{\rho_i(\omega, q) A_i}{2E'} \\ &\quad \times \sum_{j=\pm 1} j n_F(jE') (e^{(\sigma E' - \omega)\beta} + 1) \delta(E + jE' - \omega) \\ &= \pi g^2 (e^{-E\beta} + 1) \sum_{i=1}^4 \int \frac{d^3 q}{(2\pi)^3} \int_{-\infty}^{+\infty} d\omega [1 + n_B(\omega)] \frac{\rho_i(\omega, q) A_i}{2E'} \\ &\quad \times \sum_{j=\pm 1} j n_F(jE') \delta(E + jE' - \omega). \end{aligned} \quad (52)$$

Thus, using all the results, Γ in Eq. (25) is given by

$$\Gamma(E, \boldsymbol{v}) = - \frac{\pi g^2}{2E} \sum_{i=1}^4 \int \frac{d^3 q}{(2\pi)^3} \int_{-\infty}^{+\infty} d\omega [1 + n_B(\omega)] \frac{\rho_i(\omega, q) A_i}{2E'} \sum_{j=\pm 1} j n_F(jE') \delta(E + jE' - \omega). \quad (53)$$

We now simplify the above expression further by recalling that $M_Q, p \gg T$. The delta function corresponding to $j = 1$ does not contribute for $\omega \leq T$ and so can be dropped. For $E' \gg T$, the Fermi distribution function is exponentially suppressed, so that $n_F(E') \approx 0$. Employing these approximations, we have

$$\Gamma(E, \mathbf{v}) = \frac{\pi g^2}{2E} \sum_{i=1}^4 \int \frac{d^3 q}{(2\pi)^3} \int_{-\infty}^{+\infty} d\omega [1 + n_B(\omega)] \frac{\rho_i(\omega, q) A_i}{2E'} \delta(E - E' - \omega). \quad (54)$$

Furthermore, we have

$$\begin{aligned} E' &= \sqrt{(\mathbf{p} - \mathbf{q})^2 + M_Q^2} \\ &\simeq E \left(1 - \frac{2\mathbf{p} \cdot \mathbf{q}}{E^2} \right)^{1/2} \\ &\simeq E - \mathbf{v} \cdot \mathbf{q}. \end{aligned} \quad (55)$$

Although $E - E' \sim \mathcal{O}(v)$, $\frac{1}{E} - \frac{1}{E'} \sim \mathcal{O}(v^2)$, which we neglect. So, $\frac{1}{E} \approx \frac{1}{E'}$. Thus, we obtain

$$\begin{aligned} \Gamma(E, \mathbf{v}) &= \frac{\pi g^2}{2E} \sum_{i=1}^4 \int \frac{d^3 q}{(2\pi)^3} \int_{-\infty}^{+\infty} d\omega [1 + n_B(\omega)] \frac{\rho_i(\omega, q) A_i}{2E} \\ &\quad \times \delta(\omega - \mathbf{v} \cdot \mathbf{q}). \end{aligned} \quad (56)$$

IV. ENERGY LOSS AND MOMENTUM-DIFFUSION COEFFICIENTS

A. Case 1: $\mathbf{v} \parallel \mathbf{B}$

After having computed Γ , we use it to evaluate dynamic quantities such as the heavy quark energy loss and the momentum-diffusion coefficient. The HQ velocity points along \mathbf{B} , which, in turn, is taken to be of constant magnitude and pointing along \hat{z} . The energy loss of the heavy quark propagating through the high-temperature QCD plasma is given by Eq. (9). Using Eq. (54) and the approximations mentioned above, we get for the energy loss

$$\begin{aligned} \frac{dE}{dx} &= \frac{\pi g^2}{2E v} \sum_{i=1}^4 \int \frac{d^3 q}{(2\pi)^3} \int_{-\infty}^{+\infty} d\omega [1 + n_B(\omega)] \omega \frac{\rho_i(\omega, q) A_i}{2E} \\ &\quad \times \delta(\omega - \mathbf{v} \cdot \mathbf{q}), \end{aligned} \quad (57)$$

where A_i^{\parallel} are the A_i from Eqs. (34)–(37) evaluated with $v_{\perp} = 0$. For $\omega \ll T$, the Bose distribution function can be written as an expansion in ω/T so that

$$1 + n_B(\omega) \simeq \frac{T}{\omega} + \frac{1}{2} - \mathcal{O}\left(\frac{\omega}{T}\right) + \mathcal{O}\left(\frac{\omega}{T}\right)^2 - \dots \quad (58)$$

Now, the ρ_i 's in Eq. (57) are odd functions of ω [86]. Hence, only the even part of $1 + n_B(\omega)$ will contribute to the integral, since the integration over ω is symmetric. Thus, we have

$$\frac{dE}{dx} = \frac{\pi g^2}{8E^2 v} \sum_{i=1}^4 \int \frac{d^3 q}{(2\pi)^3} \int_{-\infty}^{+\infty} d\omega \omega \rho_i(\omega, q) A_i^{\parallel} \delta(\omega - \mathbf{v} \cdot \mathbf{q}). \quad (59)$$

The momentum-diffusion coefficients are given by

$$\begin{aligned} \kappa_L &= \frac{\pi g^2}{2E} \sum_{i=1}^4 \int \frac{d^3 q}{(2\pi)^3} q_L^2 \int_{-\infty}^{+\infty} d\omega [1 + n_B(\omega)] \frac{\rho_i(\omega, q) A_i}{2E} \\ &\quad \times \delta(\omega - \mathbf{v} \cdot \mathbf{q}), \end{aligned} \quad (60)$$

$$\begin{aligned} \kappa_T &= \frac{\pi g^2}{2E} \sum_{i=1}^4 \int \frac{d^3 q}{(2\pi)^3} q_T^2 \int_{-\infty}^{+\infty} d\omega [1 + n_B(\omega)] \frac{\rho_i(\omega, q) A_i}{2E} \\ &\quad \times \delta(\omega - \mathbf{v} \cdot \mathbf{q}). \end{aligned} \quad (61)$$

This time, only the odd part of $1 + n_B(\omega)$ will contribute to the integral. Thus, we have

$$\kappa_L = \frac{\pi g^2 T}{4E^2} \sum_{i=1}^4 \int \frac{d^3 q}{(2\pi)^3} q_L^2 \int_{-\infty}^{+\infty} d\omega \frac{\rho_i(\omega, q) A_i}{\omega} \delta(\omega - \mathbf{v} \cdot \mathbf{q}), \quad (62)$$

$$\kappa_T = \frac{\pi g^2 T}{4E^2} \sum_{i=1}^4 \int \frac{d^3 q}{(2\pi)^3} q_T^2 \int_{-\infty}^{+\infty} d\omega \frac{\rho_i(\omega, q) A_i}{\omega} \delta(\omega - \mathbf{v} \cdot \mathbf{q}). \quad (63)$$

Because the HQ velocity points along \mathbf{B} (hence, along \hat{z}), we have $\mathbf{v} \cdot \mathbf{q} = vq \cos \theta \equiv vq\eta$, where θ is both the angle between \mathbf{q} and the \mathbf{v} as well as the polar angle of integration. The delta function is then used to integrate over η with $d^3 q = 2\pi q^2 dq d\eta$, which sets $\omega = vq\eta$. Since $-1 \leq \eta \leq 1$, $-vq \leq \omega \leq vq$. This finally leads to

$$\frac{dE}{dx} = \frac{\pi g^2}{8E^2 v^2 (2\pi)^2} \int dq q \int_{-vq}^{vq} d\omega \omega \sum_{i=1}^4 \rho_i\left(\omega, q, \frac{\omega}{vq}\right) A_i^{\parallel}, \quad (64)$$

$$\kappa_L = \frac{\pi g^2 T}{4E^2 v} \int dq q^3 \int_{-vq}^{vq} d\omega \sum_{i=1}^4 \frac{\rho_i\left(\omega, q, \frac{\omega}{vq}\right) A_i^{\parallel}}{\omega} \left(\frac{\omega^2}{v^2 q^2}\right), \quad (65)$$

$$\kappa_T = \frac{\pi g^2 T}{4E^2 v} \int dq q^3 \int_{-vq}^{vq} d\omega \sum_{i=1}^4 \frac{\rho_i(\omega, q, \frac{\omega}{vq}) A_i^\parallel}{\omega} \left(1 - \frac{\omega^2}{v^2 q^2}\right). \quad (66)$$

B. Case 2: $\mathbf{v} \perp \mathbf{B}$

The HQ velocity now lies in the x - y plane, with the magnetic field pointing in the \hat{z} direction as earlier. Since \mathbf{v} is no longer oriented along the z axis, $\mathbf{v} \cdot \mathbf{q}$ is not trivial. The direction of HQ velocity in the x - y plane can be specified by the azimuthal angle ϕ' (the polar angle $\theta' = 0$, as it is in the x - y plane). The vector \mathbf{q} is specified by q , θ , and ϕ (our integration variables), where θ is the polar angle and ϕ is the azimuthal angle. Then,

$$\mathbf{v} \cdot \mathbf{q} = vq \sin \theta \cos(\phi - \phi'), \quad (67)$$

where $v = |\mathbf{v}|$, $q = |\mathbf{q}|$. The interaction rate becomes¹

$$\begin{aligned} \Gamma(E, \mathbf{v}) &= \frac{\pi g^2}{4E^2 (2\pi)^3} \sum_{i=1}^4 \int dq \int_0^\pi d\theta \sin \theta \\ &\times \int_0^{2\pi} d\phi \int_{-\infty}^{+\infty} d\omega [1 + n_B(\omega)] \\ &\times \rho_i(\omega, q) A_i^\perp \delta[\omega - vq \sin \theta \cos(\phi - \phi')], \quad (68) \end{aligned}$$

where A_i^\perp are the A_i from Eqs. (34)–(37) evaluated with $v_z = 0$. We introduce a variable $y = \phi - \phi'$. Γ then simplifies to

$$\begin{aligned} \Gamma(E, \mathbf{v}) &= \frac{g^2}{32E^2 v^3 \pi^2} \int dq q \int_0^\pi d\theta \sin \theta \delta\left(\sin \theta - \frac{\omega}{vq \cos y}\right) \\ &\times \int_{-\phi'}^{2\pi - \phi'} \frac{dy}{\cos y} \int_{-\infty}^{+\infty} d\omega [1 + n_B(\omega)] \\ &\times \sum_{i=1}^4 A_i^\perp \rho_i(\omega, q). \quad (69) \end{aligned}$$

We use the result

$$\int_0^\pi d\theta \sin \theta \delta(\sin \theta - c) = \frac{2c}{\sqrt{1-c^2}} \Theta(c) \Theta(1-c), \quad c \in \mathbb{R}, \quad (70)$$

to integrate over θ . The Θ function sets

$$\begin{aligned} 0 &\leq \frac{\omega}{vq \cos y} \leq 1, \\ 0 &\leq \omega \leq vq \cos y. \quad (71) \end{aligned}$$

Γ then finally becomes

$$\begin{aligned} \Gamma(E, \mathbf{v}) &= \frac{g^2}{16E^2 v^3 \pi^2} \int dq \int_{-\phi'}^{2\pi - \phi'} dy \int_0^{vq \cos y} d\omega \\ &\times \frac{q}{\sqrt{v^2 q^2 \cos^2 y / \omega^2 - 1}} \frac{[1 + n_B(\omega)]}{\cos y} \sum_{i=1}^4 A_i^\perp \rho_i(\omega, q). \quad (72) \end{aligned}$$

From Eqs. (22)–(24), the momentum-diffusion coefficients are obtained as

$$\begin{aligned} \kappa_1 &= \frac{g^2}{16E^2 v^3 \pi^2} \int dq \int_{-\phi'}^{2\pi - \phi'} dy \int_0^{vq \cos y} d\omega \\ &\times \frac{\omega^3 \cos^2(y + \phi') [1 + n_B(\omega)]}{\cos^3 y \sqrt{v^2 q^2 \cos^2 y - \omega^2}} \sum_{i=1}^4 A_i^\perp \rho_i(\omega, q), \quad (73) \end{aligned}$$

$$\begin{aligned} \kappa_2 &= \frac{g^2}{16E^2 v^3 \pi^2} \int dq \int_{-\phi'}^{2\pi - \phi'} dy \int_0^{vq \cos y} d\omega \\ &\times \frac{\omega^3 \sin^2(y + \phi') [1 + n_B(\omega)]}{\cos^3 y \sqrt{v^2 q^2 \cos^2 y - \omega^2}} \sum_{i=1}^4 A_i^\perp \rho_i(\omega, q), \quad (74) \end{aligned}$$

$$\begin{aligned} \kappa_3 &= \frac{g^2}{16E^2 v^3 \pi^2} \int dq \int_{-\phi'}^{2\pi - \phi'} dy \int_0^{vq \cos y} d\omega \\ &\times \frac{q\omega \sqrt{v^2 q^2 \cos^2 y - \omega^2} [1 + n_B(\omega)]}{\cos^3 y} \sum_{i=1}^4 A_i^\perp \rho_i(\omega, q). \quad (75) \end{aligned}$$

Also, the HQ energy loss [from Eq. (9)] comes out to be

$$\begin{aligned} dE/dx &= \frac{g^2}{16E^2 v^2 \pi^2} \int dq \int_{-\phi'}^{2\pi - \phi'} dy \int_0^{vq \cos y} d\omega \\ &\times \frac{\omega^2 q [1 + n_B(\omega)]}{\cos y \sqrt{v^2 q^2 \cos^2 y - \omega^2}} \sum_{i=1}^4 A_i^\perp \rho_i(\omega, q). \quad (76) \end{aligned}$$

V. RESULTS AND DISCUSSIONS

In this section, we present the results of the heavy quark (charm and bottom) momentum-diffusion coefficients and the heavy quark energy loss. The running coupling constant is taken up to one loop:

$$g(\Lambda) = \left[\frac{48\pi^2}{(33 - 2N_f) \ln\left(\frac{\Lambda^2}{\Lambda_{\overline{\text{MS}}}}\right)} \right]^{1/2}. \quad (77)$$

The renormalization scale Λ can be taken to be $2\pi T$ to introduce temperature dependence in the coupling. The $\overline{\text{MS}}$ scale is taken to be 176 MeV [87]. The use of this form of the coupling is justified, since $q_f B \ll T^2$. In the strong field limit, use of momentum-dependent couplings might be

¹The limits of the q integration are discussed in the next section.

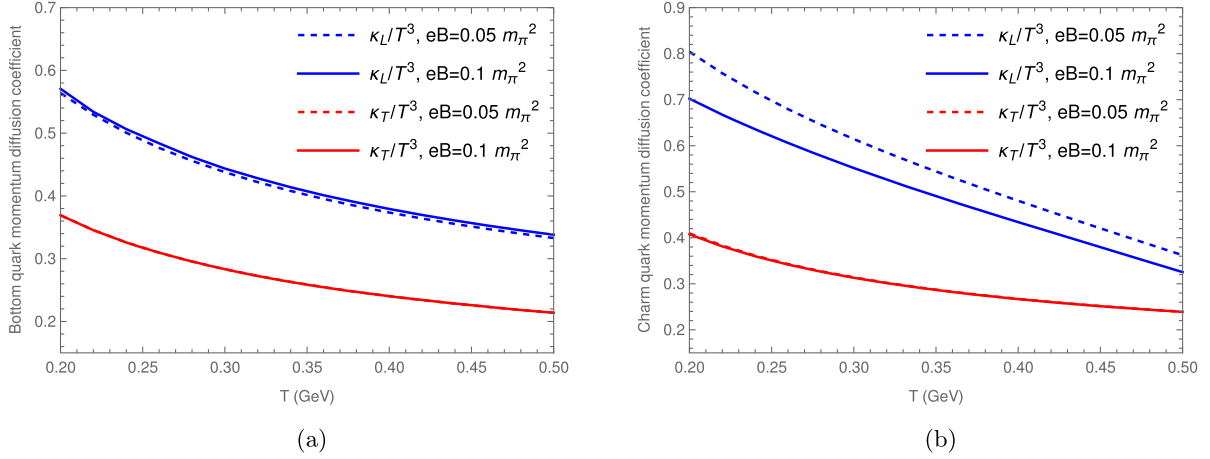


FIG. 5. Normalized momentum-diffusion coefficients for bottom (a) and charm (b) quarks as a function of temperature at different fixed values of background magnetic field.

more appropriate [88]. The bottom and charm quark masses are taken to be 4.18 and 1.28 GeV, respectively. The HQ momentum is taken to be $p = 0.3$ GeV. Heavy quark dynamics with temperature-dependent couplings was studied first in [60].

An important point to note is that the integrals in Eqs. (64)–(66) are logarithmically UV divergent and, hence, require a UV cutoff. Following the prescription of [89], we take the UV cutoff to be $3.1Tg^{1/3}$. The reason for this divergence is that our calculations are confined to the region of soft gauge boson momentum transfer. In the $B = 0$ case, it is shown explicitly that the dependence on this cutoff vanishes once the full range of momentum transfers is taken into account. We expect the same to be true in the case of weak magnetic fields, too. However, the full calculation, including hard scatterings, is left for future work. As mentioned earlier, the soft scatterings contribute to $\mathcal{O}(g(T)^2)$ in Γ , whereas the hard contribution to Γ will be of $\mathcal{O}(g(T)^4)$. As such, it can be inferred that the major contribution to the momentum diffusion of the HQ via elastic scatterings comes from soft gluon exchange with the thermal quarks and gluons of the heat bath. It is also worth mentioning that this UV cutoff is not necessary if one uses the lowest Landau level approximation for the HQ propagator in the presence of a strong ($q_f B \gg T^2$) magnetic field, because of the appearance of the exponential factor $e^{-k_\perp^2/|q_f B|}$ in the HQ propagator.

A. Case 1: $\mathbf{v} \parallel \mathbf{B}$

Figures 5 and 6 show the temperature variation of the momentum-diffusion coefficients ($\kappa_{L/T}$) for heavy quarks at a fixed momentum [$p = 0.3$ GeV]. For comparison, the $B = 0$ results are also shown in Fig. 6. As can be seen from Figs. 5(a) and 5(b), both the longitudinal and transverse momentum-diffusion coefficients show a monotonic decrease with temperature. For bottom quark, the magnitude

of the longitudinal component is ~ 1.5 times larger than its transverse counterpart in the entire temperature range. For the charm quark, κ_L/κ_T is much larger (~ 2) at lower temperatures than at higher temperatures (~ 1.5). The figures also show the behavior of the coefficients with magnetic field. κ_T (normalized) for both the heavy flavors show very little sensitivity to changes in the magnetic field. In the case of κ_L , there is a strong dependence on B strength for the charm quark, which increases with decreasing field strength. For the bottom quark, however, both κ_L and κ_T decrease with decreasing B . Figure 6 shows the $B = 0$ result for the momentum-diffusion coefficients. The momentum diffusion of charm quarks is faster than that of the bottom quark, owing to the smaller mass of the former. κ_T is larger than κ_L in the entire temperature range, for both the heavy flavors. Also, the degree of anisotropy is negligible in the case of the bottom quark, whereas it is discernible in the case of the

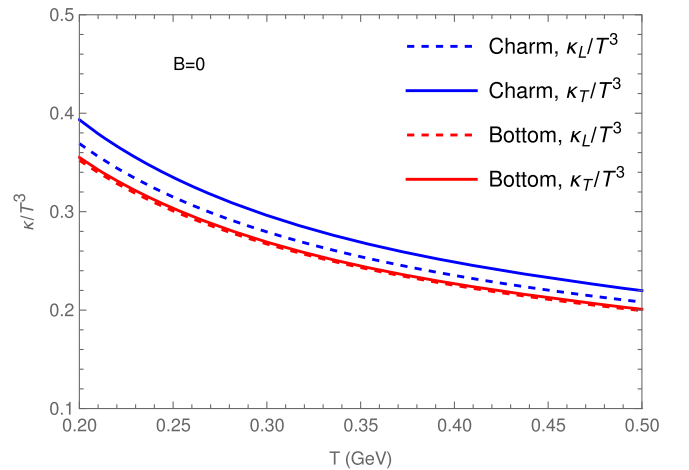


FIG. 6. Normalized transverse and longitudinal momentum-diffusion coefficients for both charm and bottom quarks as a function of temperature in the absence of a background magnetic field.

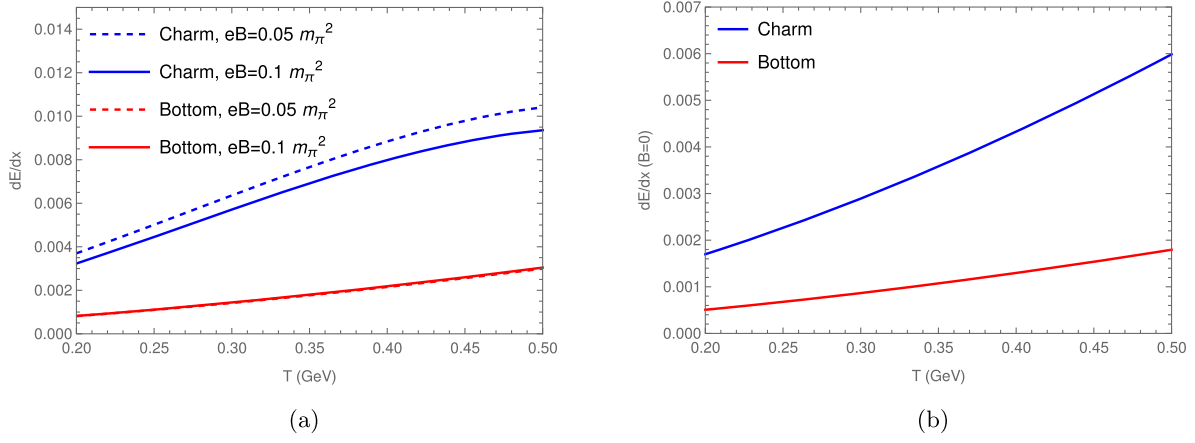


FIG. 7. (a) Energy loss of heavy quark as a function of temperature in the presence of fixed values of background magnetic field of strengths. (b) Energy loss of heavy quarks in the absence of a background magnetic field.

charm quark. A large value of the momentum-diffusion coefficient would work toward decreasing the yield of bound states such as the J/ψ (charmonium), bottomonium, etc., the Brownian motion of the heavy quarks overwhelming the screened potential holding the $q - \bar{q}$ pair together. On the other hand, a stronger energy loss, dE/dx , of the propagating HQ would result in the stopping of a $q - \bar{q}$ pair (not so much for $b - \bar{b}$), leading to the increase in yield of mesonic bound states involving heavy quarks. The fate of a $q - \bar{q}$ pair produced in the initial stages of a heavy-ion collision, thus, depends on these competing factors. This phenomenon has been elucidated in detail in [90].

Figure 7(a) shows the temperature variation of the HQ (bottom and charm) energy loss in the presence of a weak constant background field. In contrast to the momentum-diffusion coefficients, the energy loss records an increasing trend with temperature. The sensitivity of the energy loss to temperature is greater for the charm quark because of its smaller mass as compared to the bottom quark. The sensitivity to magnetic field is also greater for the charm quark compared to the bottom quark, which is reflected in Fig. 7(a) by the discernible curves at $eB = 0.05 m_\pi^2$ and $eB = 0.1 m_\pi^2$. With regards to variation of HQ energy loss with magnetic field, the charm quark again records an opposite trend compared to the bottom quark, wherein the former decreases with increasing B , while the latter increases. Figure 7(b) shows the variation of HQ energy loss with temperature in the absence of a background magnetic field. The temperature variation is the same as in the finite B case, with both the magnitude as well as the rate of increase being greater for the charm quark. Again, this can be attributed to the lighter mass of the charm quark compared to the bottom.

B. Case 2: $\mathbf{v} \perp \mathbf{B}$

In the case of $\mathbf{v} \perp \mathbf{B}$, we have three momentum-diffusion coefficients κ_1 , κ_2 , and κ_3 . In Figs. 8(a) and 8(b), we show

the variation of κ_1 , κ_2 , and κ_3 with T at fixed values of the background magnetic field strength. For both the charm and bottom quarks, the κ_1 coefficient magnitude is significantly larger (~ 2 times) than κ_2 and κ_3 . Also, like in the $\mathbf{v} \parallel \mathbf{B}$ case, the charm quark coefficients are larger in magnitude than their bottom quark counterparts. Overall, the momentum-diffusion coefficients are smaller in magnitude than in the case of $\mathbf{v} \parallel \mathbf{B}$. Figures 8(c) and 8(d) focus on the effect of magnetic field strength on the temperature variation of charm and bottom quark momentum-diffusion coefficients, respectively. As is evident, the curves corresponding to different magnetic field strengths almost overlap. The variation with magnetic field strength is very feeble ($\sim 0.1\%$) for both the charm and bottom quarks. The momentum-diffusion coefficients in this case are, therefore, much less sensitive to changes in magnetic field strength compared to the $\mathbf{v} \parallel \mathbf{B}$ case.

To specify the direction of HQ velocity, one needs to fix the value of ϕ' . Figures 8–10 have been obtained with $\phi' = 0$. From Eqs. (73) and (74), one can see that setting $\phi' = \pi/2$ leads to the following condition on the integrands²:

$$\begin{aligned} \kappa_1(\phi' = \pi/2) &= \kappa_2(\phi' = 0), \\ \kappa_2(\phi' = \pi/2) &= \kappa_1(\phi' = 0). \end{aligned} \quad (78)$$

The condition (78) can be seen in Figs. 9(a) and 9(b), where the blue and green curves are interchanged. It should be pointed out that this happens primarily because of the factors $\cos^2(y + \phi')$ and $\sin^2(y + \phi')$ in the κ_1 and κ_2 integrals

²The limits of y integration are ϕ' dependent, which also change as one changes ϕ' . Thus, strictly, the equality in Eq. (78) holds only for the integrand, not for the integral. However, the value of the integral depends very weakly on the limits of the y integration, so that the final numerical values postintegration satisfy Eq. (78) up to five significant figures after the decimal point.

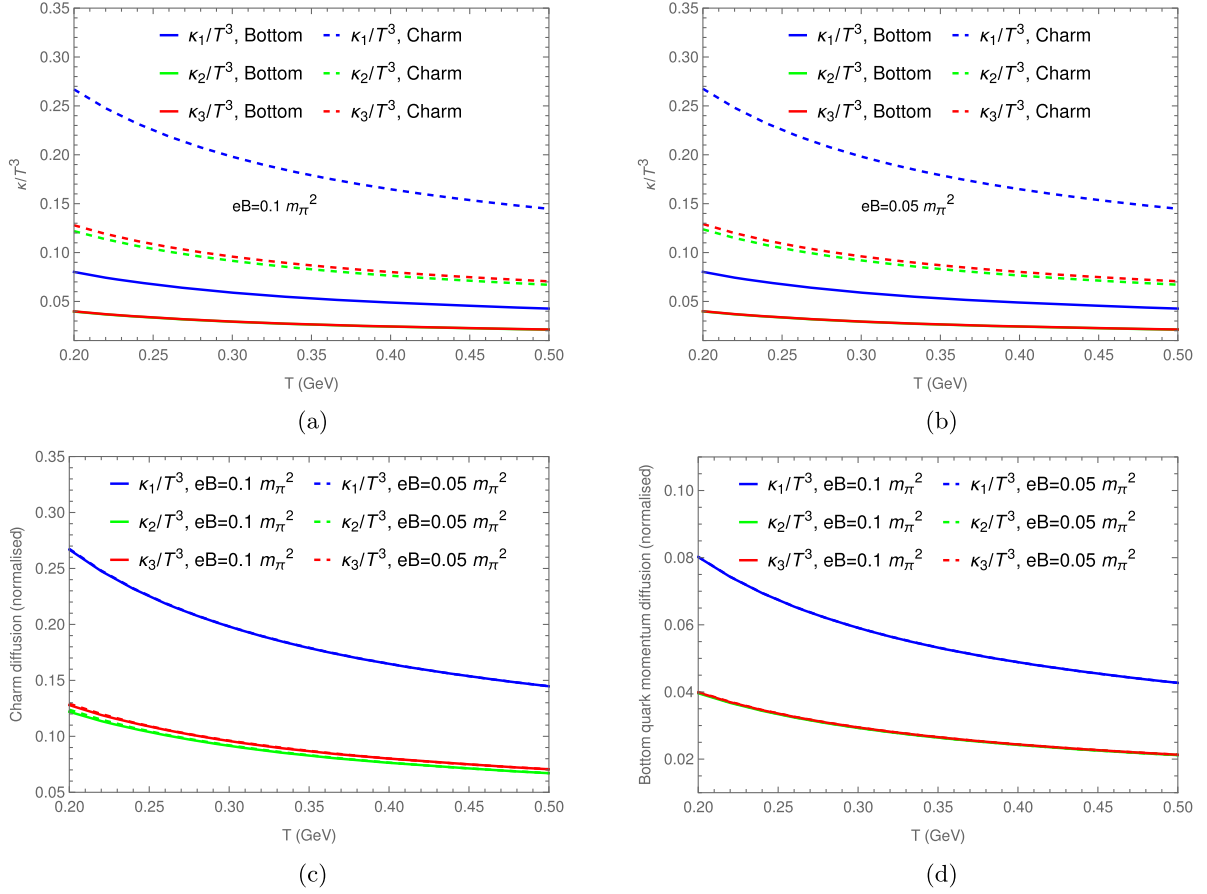


FIG. 8. (a) Temperature variation of normalized momentum-diffusion coefficients of both bottom and charm quarks at $eB = 0.1 m_\pi^2$. (b) The same as (a) but at $eB = 0.05 m_\pi^2$. (c) Temperature variation of charm quark normalized momentum-diffusion coefficients at different values of magnetic field strength. (d) The same as (c) but for the bottom quark.

[Eqs. (73) and (74)]. Physically, $\phi' = 0$ and $\phi' = \pi/2$ correspond to the HQ velocity pointing toward $+\hat{x}$ and $+\hat{y}$, respectively. Also, κ is a measure of mean squared momentum transfer between the HQ and the light thermal particles of the medium [56], so that $\kappa_{1/2/3}$ [as defined in

Eqs. (22)–(24)] is a measure of the mean square of the $x/y/z$ component of the transfer momentum. One can observe from Figs. 9(a) and 9(b) that, when the HQ velocity points purely in the $+\hat{x}$ direction ($\phi' = 0$), κ_1 is the largest. Similarly, when \mathbf{v} points along $+\hat{y}$ ($\phi' = \pi/2$), κ_2 is the largest.

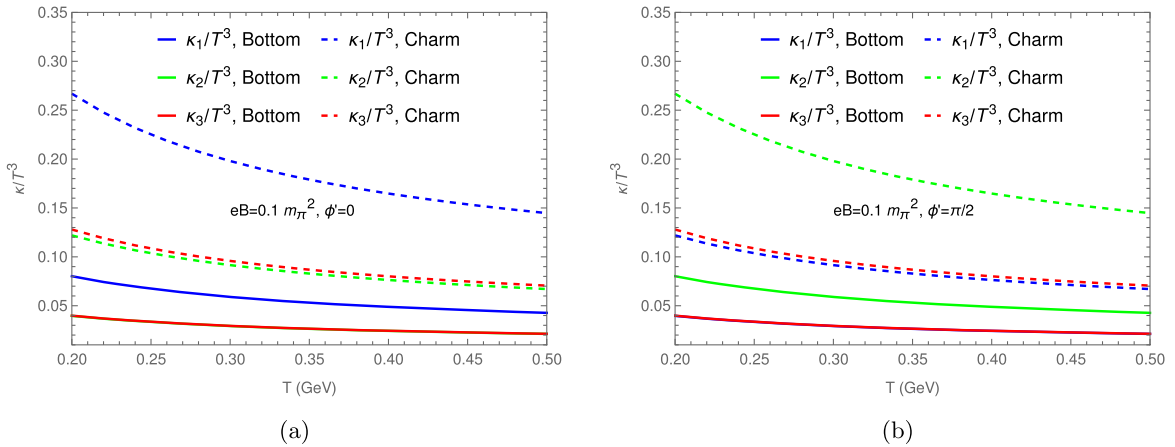


FIG. 9. ϕ' dependence of κ 's. (a) Momentum-diffusion coefficients of both charm and bottom quarks at $\phi' = 0$ and $eB = 0.1 m_\pi^2$. (b) Momentum-diffusion coefficients of both charm and bottom quarks at $\phi' = \pi/2$ and $eB = 0.1 m_\pi^2$.

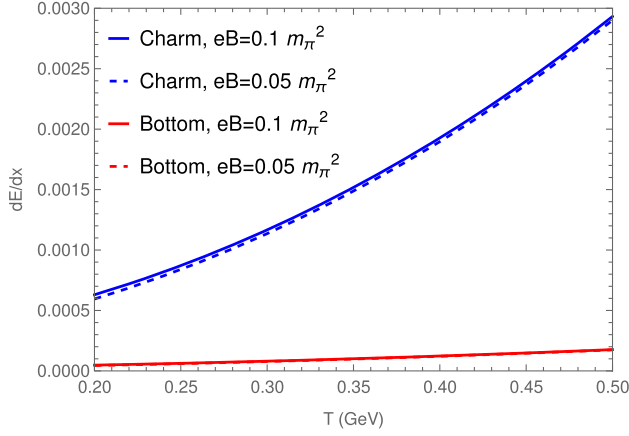


FIG. 10. Energy loss of both bottom and charm quarks at different values of background magnetic field strengths.

This suggests that the momentum transfer between the HQ and the medium happens preferentially along the direction of HQ velocity.

Figure 10 shows the variation of energy loss of both charm and bottom quarks with T and also their dependence on magnetic field strength. Similar to case 1, the energy loss is an increasing function of T , where both the magnitude and the rate of increase are greater for the charm quark, compared to bottom quark. Compared to case 1, the sensitivity to changes in magnetic field strength is smaller; the charm quark values decrease by an average of 2.45% as one goes from $eB = 0.1m_\pi^2$ to $eB = 0.05m_\pi^2$, while the corresponding value for the bottom quark is 2.74%. Compared to the case of $\mathbf{v} \parallel \mathbf{B}$, the charm quark energy loss for $\mathbf{v} \perp \mathbf{B}$ is on an average smaller by 76.8%. The bottom quark values for case 2 are also smaller than those of case 1, on an average, by 94.3%.

VI. APPLICATION: SPATIAL DIFFUSION COEFFICIENT

As mentioned in Sec. II, the drag coefficient η can be obtained from the momentum-diffusion coefficient via the fluctuation dissipation relation:

$$\eta_D = \frac{\kappa}{2M_Q T}. \quad (79)$$

The zero momentum value of the drag coefficient is then obtained from the zero momentum value of the momentum-diffusion coefficient:

$$\eta_D(p=0) = \frac{\kappa(p=0)}{2M_Q T}. \quad (80)$$

The spatial diffusion coefficient D_s can be defined via $\eta_D(p=0)$ as [12]

$$D_s = \frac{T}{\eta_D(p=0)M_q}. \quad (81)$$

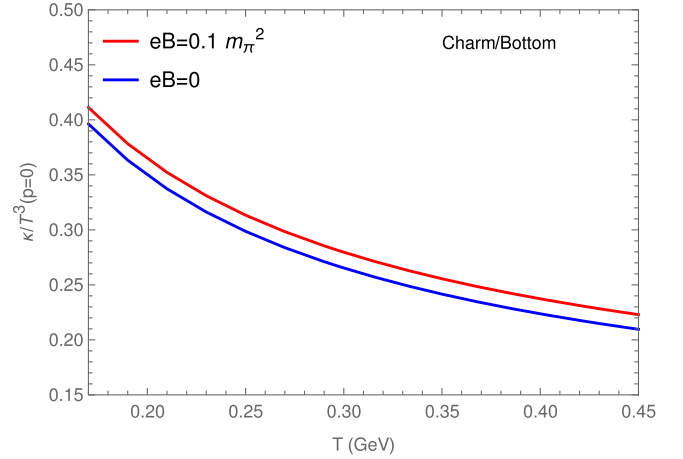


FIG. 11. Normalized transverse and longitudinal momentum-diffusion coefficients in the static limit ($\omega \rightarrow 0$) for both charm and bottom quarks as a function of temperature in the presence and absence of a background magnetic field.

To evaluate $\kappa(p=0)$, we execute $p=0$ in the delta functions of Eqs. (62) and (63), which leads to $\omega=0$. So, we have to calculate the momentum-diffusion coefficients in the $\omega \rightarrow 0$ limit:

$$\sum_{i=1}^4 \frac{\rho_i(\omega, q) A_i(\omega, q)}{\omega} \Big|_{\omega \rightarrow 0} = \frac{A_1 \rho_1}{\omega} \Big|_{\omega \rightarrow 0}. \quad (82)$$

All other terms vanish due to either the A_i 's or ρ_i 's vanishing in the $\omega \rightarrow 0$ limit. Finally, we are left with

$$\begin{aligned} \kappa_L &= \frac{1}{2} \frac{\pi g^2 T}{4M_Q^2 (2\pi)^2} \int_0^{q_{\max}} dq \int_0^\pi d\theta \frac{A_1(\omega=0) q^4}{\pi [q^4 + q^2 \text{Re}_b(\omega=0)]^2} \\ &\quad \times (q^4 \sin^3 \theta) \frac{\text{Im}_b}{\omega} \Big|_{\omega \rightarrow 0}, \end{aligned} \quad (83)$$

$$\begin{aligned} \kappa_T &= \frac{\pi g^2 T}{4M_Q^2 (2\pi)^2} \int_0^{q_{\max}} dq \int_0^\pi d\theta \frac{A_1(\omega=0) q^4}{\pi [q^4 + q^2 \text{Re}_b(\omega=0)]^2} \\ &\quad \times (q^4 \sin \theta \cos^2 \theta) \frac{\text{Im}_b}{\omega} \Big|_{\omega \rightarrow 0}. \end{aligned} \quad (84)$$

The important thing to note is that $A_1(\omega=0) = M_Q^2$ and, hence, the HQ mass dependence vanishes in κ_L and κ_T . Thus, we expect the momentum-diffusion coefficient values for the charm and bottom quarks to be identical.

The momentum-diffusion coefficient curves for the charm and bottom quarks overlap, as expected (Fig. 11). However, the longitudinal and transverse components are also indistinguishable. Hence, when the heavy quarks are static, the momentum diffusion of HQ is isotropic, even in the presence of a background magnetic field.

The case is similar for the spatial diffusion coefficient D_s as well. From Eqs. (80) and (81), it can be seen that the HQ

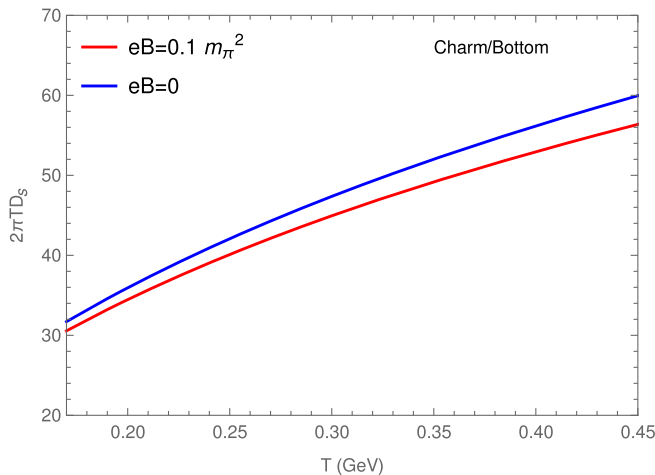


FIG. 12. Spatial diffusion coefficient D_s (multiplied with $2\pi T$) as a function of temperature in the presence and absence of a background weak magnetic field.

mass dependence cancels in D_s . In fact, this is one of the reasons why HQ diffusion is believed to carry generic information about the QCD medium.

Figure 12 shows the variation of the scaled spatial diffusion coefficient ($2\pi TD_s$) with temperature in the presence of a background magnetic field of strength $eB = 0.1m_\pi^2$. For comparison, the $B = 0$ curve is also plotted. The curves corresponding to the charm and bottom quarks overlap, as expected. As can be seen, the spatial diffusion coefficient decreases in the presence of a magnetic field. This simply means that the mean squared momentum transfer per unit time between the HQ and the light partons (of which κ is a measure) increases in the presence of a weak magnetic field, compared to $B = 0$. The increasing trend with temperature is similar to what has been observed in several pQCD leading-order studies in the past, with both T -dependent and T -independent couplings [13,56,90].

VII. SUMMARY AND CONCLUSIONS

In this work, we have investigated the dynamics of heavy quarks, viz. charm and bottom in the presence of a weak background magnetic field. In particular, we have calculated the momentum-diffusion coefficients and the energy loss perturbatively up to first order in the strong coupling α_s . The interaction rate is calculated by considering $2 \rightarrow 2$ elastic collisions of the form $Qq \rightarrow Qq$ and $Qg \rightarrow Qg$, by calculating the imaginary part of the heavy-quark self-energy which is related to the squared matrix elements of the aforementioned collisional processes via the cutting rules. Gluon bremsstrahlung and Compton scattering processes are neglected, since the former contributes only at higher order in α_s and the contribution of the latter is suppressed by powers of M_Q/T . There is a logarithmic UV divergence present in the results of both the momentum-diffusion coefficients and the energy loss. This is due to the

fact that, in this work, as a first attempt, we have calculated the contribution to the dynamical quantities arising out of only soft gluon exchange. It should, however, be remembered that the interaction rate is indeed dominated by processes involving soft gluon exchanges and hard scatterings contribute only at higher orders. In future, we shall include the hard scatterings, too, to get rid of the aforementioned UV cutoff.

We have investigated the temperature dependence of the momentum diffusion coefficients and energy loss for both the heavy flavors, for two cases: (1) $\mathbf{v} \parallel \mathbf{B}$ and (2) $\mathbf{v} \perp \mathbf{B}$. In the former case, we define two momentum-diffusion coefficients κ_L and κ_T , whereas in the latter, we have three such coefficients: κ_1 , κ_2 , and κ_3 . The temperature behavior of all the coefficients is similar in that the normalized coefficient magnitudes decrease with T .

For case 1, κ_T for both the flavors decreases with T at the same rate, while κ_L decreases faster for charm. For the values of magnetic fields considered, the sensitivity of charm quark diffusion coefficients to the magnetic field is found to be greater than that of the bottom quark, possibly owing to the larger mass of the former. Furthermore, the effect of increasing the magnetic field strength seems to have the opposite effects on the magnitudes of the charm and bottom diffusion coefficients; while the former decreases, the latter records an increase. For comparison, the $B = 0$ results of the momentum-diffusion coefficient (κ) have also been shown. It can be seen that the degree of anisotropy is much larger for the charm quark than that of the bottom quark, which suggests that the mass of the heavy quark under consideration plays a strong role in determining the isotropicity of κ . For each of the flavors, κ_L/T^3 is found to be more sensitive to the magnetic field strength as compared to κ_T/T^3 . The heavy flavor energy loss is an increasing function of the temperature, in both the presence and absence of a background magnetic field. Again, owing to its lighter mass, the sensitivity to both temperature and magnetic field is greater for the charm quark, whereas for the bottom quark, the curves corresponding to different magnetic fields almost overlap. The $B = 0$ results are similar with the rate of increase of the charm quark energy loss being steeper.

For case 2, we observe certain similarities as well as differences *vis-à-vis* observations of case 1. For instance, similar to case 1, the rate of variation of κ with T is greater for charm, compared to bottom. Sensitivity of coefficient magnitudes to magnetic field strength is, however, much less for both the flavors in comparison with case 1. For both the flavors, κ_2 and κ_3 magnitudes, for $\phi' = 0$, are almost similar for the entire temperature range (the similarity is more for bottom), which, in turn, is significantly less than the κ_1 values. Thus, for $\phi' = 0$, we have $|\kappa_1/T^3| > |\kappa_2/T^3| \approx |\kappa_3/T^3|$. Similarly, for $\phi' = \pi/2$, we obtain $|\kappa_2/T^3| > |\kappa_1/T^3| \approx |\kappa_3/T^3|$. Such a hierarchy in coefficient magnitudes, where two of the coefficients are almost of the same magnitude,

which, in turn, are significantly different from the third, is also seen in [52]. The HQ energy loss exhibits a significant reduction in magnitude in comparison to case 1. The charm quark energy loss is on average smaller by 76.8%, whereas the bottom quark values for case 2 are smaller than those of case 1, on average, by 94.3%. Similar to case 1, however, the rate of increase of energy loss with T is significantly larger for the charm quark, as compared to the bottom quark.

We have also looked at the $p = 0$ (static limit) results of momentum-diffusion coefficients of the heavy quarks and found that the anisotropy in κ completely vanishes in the said limit. Using this, we have looked at the spatial diffusion (D_s) of HQ. Interestingly, the HQ mass dependence cancels out in both $\kappa(p = 0)$ and D_s .

ACKNOWLEDGMENTS

D. D. acknowledges the help of Aritra Bandyopadhyay received in the course of fruitful discussions. D. D. also acknowledges the help received from Bithika Karmakar with regards to certain calculations pertaining to the evaluation of the resummed gluon propagator. D. D. is grateful to Abhishek Tiwary for checking several results presented here. D. D. also thanks Sumit for help in drawing Feynman diagrams.

APPENDIX A: TENSOR STRUCTURE OF RESUMMED GLUON PROPAGATOR IN THE PRESENCE OF A MAGNETIC FIELD

We begin by discussing the four-vectors that characterize the system under consideration. The fluid 4-velocity in local rest frame (LRF) and the metric tensor is given by

$$u^\mu = (1, 0, 0, 0), \quad g^{\mu\nu} = \text{diag}(1, -1, -1, -1). \quad (\text{A1})$$

The direction of the external magnetic field is specified by the projection of the EM field tensor $F^{\mu\nu}$ along u^μ :

$$n_\mu = \frac{1}{2B} \epsilon_{\mu\nu\rho\lambda} u^\nu F^{\rho\lambda} = (0, 0, 0, 1). \quad (\text{A2})$$

Introduction of these four-vectors allows one to define a Lorentz-invariant energy and momentum component as

$$q^0 = q_0 = Q \cdot u, \quad q^3 = -q_3 = Q \cdot n. \quad (\text{A3})$$

We define parallel and perpendicular components of vectors and the metric tensor in the LRF as

$$Q_\parallel^\mu = (Q \cdot u) u^\mu + (Q \cdot n) n^\mu = (q^0, 0, 0, q^3), \quad (\text{A4})$$

$$Q_\perp^\mu = Q^\mu - Q_\parallel^\mu = (0, q^1, q^2, 0), \quad (\text{A5})$$

$$Q_\parallel^2 = q_0^2 - q_3^2, \quad Q_\perp^2 = -(q_1^2 + q_2^2) = -q_\perp^2, \quad (\text{A6})$$

$$g_\parallel^{\mu\nu} = u^\mu u^\nu - n^\mu n^\nu = \text{diag}(1, 0, 0, -1), \quad (\text{A7})$$

$$g_\perp^{\mu\nu} = g^{\mu\nu} - g_\parallel^{\mu\nu} = \text{diag}(0, -1, -1, 0). \quad (\text{A8})$$

One can further redefine u^μ and n^μ , respectively, as

$$\bar{u}^\mu = u^\mu - \frac{(Q \cdot u) Q^\mu}{Q^2} = u^\mu - \frac{q_0 Q^\mu}{Q^2}, \quad (\text{A9})$$

$$\bar{n}^\mu = n^\mu - \frac{(\tilde{Q} \cdot n) \tilde{Q}^\mu}{\tilde{Q}^2} = n^\mu - \frac{q_3 Q^\mu}{q^2} + \frac{q_0 q_3 u^\mu}{q^2}, \quad (\text{A10})$$

where $\tilde{Q}^\mu = Q^\mu - (Q \cdot u) u^\mu$. \bar{u}^μ and \bar{n}^μ so defined are orthogonal to Q^μ and \tilde{Q}^μ , respectively. In the presence of a magnetic field, a set of basis tensors that are mutually orthogonal, can be constructed out of the four-vectors mentioned above:

$$\Delta_1^{\mu\nu} = \frac{\bar{u}^\mu \bar{u}^\nu}{\bar{u}^2}, \quad (\text{A11})$$

$$\Delta_2^{\mu\nu} = g_\perp^{\mu\nu} - \frac{Q_\perp^\mu Q_\perp^\nu}{Q_\perp^2}, \quad (\text{A12})$$

$$\Delta_3^{\mu\nu} = \frac{\bar{n}^\mu \bar{n}^\nu}{\bar{n}^2}, \quad (\text{A13})$$

$$\Delta_4^{\mu\nu} = \frac{\bar{u}^\mu \bar{n}^\nu + \bar{u}^\nu \bar{n}^\mu}{\sqrt{\bar{u}^2} \sqrt{\bar{n}^2}}. \quad (\text{A14})$$

These tensors satisfy the following properties:

$$(\Delta_4)^{\mu\rho} (\Delta_4)_{\rho\nu} = (\Delta_1)_\nu^\mu + (\Delta_3)_\nu^\mu, \quad (\text{A15})$$

$$(\Delta_k)^{\mu\rho} (\Delta_4)_{\rho\nu} + (\Delta_4)^{\mu\rho} (\Delta_k)_{\rho\nu} = (\Delta_4)_\nu^\mu, \quad (\text{A16})$$

$$(\Delta_2)^{\mu\rho} (\Delta_4)_{\rho\nu} = (\Delta_4)^{\mu\rho} (\Delta_2)_{\rho\nu} = 0. \quad (\text{A17})$$

Any second-rank tensor can be expanded in terms of these basis tensors. As such, the gluon self-energy can be written as

$$\Pi^{\mu\nu}(q_0, \mathbf{q}) = b(q_0, \mathbf{q}) \Delta_1^{\mu\nu} + c(q_0, \mathbf{q}) \Delta_2^{\mu\nu} + d(q_0, \mathbf{q}) \Delta_3^{\mu\nu} + a(q_0, \mathbf{q}) \Delta_4^{\mu\nu}, \quad (\text{A18})$$

where, b , c , d , and a are Lorentz-invariant form factors. The Schwinger-Dyson equation relates the bare propagator, resummed propagator, and the self-energy of the particle under consideration. For the gluon propagator, we have

$$\mathcal{D}_{\mu\nu}^{-1} = \mathcal{D}_{\mu\nu}^0 - \Pi_{\mu\nu}, \quad (\text{A19})$$

where $\mathcal{D}_{\mu\nu}^0$ is the bare gluon propagator. We recall that any rank-2 tensor (and its inverse) can be written in terms of the basis tensors Δ'_i 's. Then, using Eqs. (A18) and (A19) and

the fact that $\mathcal{D}_{\mu\rho}^{-1}\mathcal{D}^{\rho\nu} = g_{\mu}^{\nu}$, we can derive the structure of the resummed gluon propagator as mentioned in Eq. (28).

APPENDIX B: FORM FACTORS IN A WEAK MAGNETIC FIELD

The fermion propagator in a weak background magnetic field is written as a series expansion in powers of qB as [up to $\mathcal{O}(qB)^2$]

$$\begin{aligned} iS(K) &= i\frac{(K+m_f)}{K^2-m_f^2} - q_f B \frac{\gamma_1\gamma_2(K_{\parallel}+m_f)}{(K^2-m_f^2)^2} \\ &\quad - 2i(q_f B)^2 \frac{[K_{\perp}^2(K_{\parallel}+m_f) + K_{\perp}(m_f^2-K_{\parallel}^2)]}{(K^2-m_f^2)^4} \\ &\equiv S_0(K) + S_1(K) + S_2(K). \end{aligned}$$

The quark loop (fermion) contribution to the gluon self-energy is then given by

$$\begin{aligned} \Pi_f^{\mu\nu}(Q) &= -\sum_f \frac{ig^2}{2} \int \frac{d^4K}{(2\pi)^4} \text{Tr}[\gamma^{\nu}\{S_0(K) + S_1(K) + S_2(K)\} \\ &\quad \times \gamma^{\mu}\{S_0(P) + S_1(P) + S_2(P)\}] \\ &= \Pi_{(0,0)}^{\mu\nu}(Q) + \Pi_{(1,1)}^{\mu\nu}(Q) + 2\Pi_{(2,0)}^{\mu\nu}(Q) + \mathcal{O}[(q_f B)^3], \end{aligned}$$

where the first term is of $\mathcal{O}(qB)$ and the remaining are of $\mathcal{O}((qB)^2)$. The $\mathcal{O}(qB)$ term vanishes owing to Furry's theorem. The nonvanishing terms are given as

$$\Pi_{(0,0)}^{\mu\nu}(Q) = \sum_f i2g^2 \int \frac{d^4K}{(2\pi)^4} \frac{[P^{\mu}K^{\nu} + K^{\mu}P^{\nu} - g^{\mu\nu}(K \cdot P - m_f^2)]}{(K^2 - m_f^2)(P^2 - m_f^2)}, \quad (\text{B1})$$

$$\Pi_{(1,1)}^{\mu\nu}(Q) = \sum_f 2ig^2(q_f B)^2 \int \frac{d^4K}{(2\pi)^4} \frac{[P_{\parallel}^{\mu}K_{\parallel}^{\nu} + K_{\parallel}^{\mu}P_{\parallel}^{\nu} + (g_{\parallel}^{\mu\nu} - g_{\perp}^{\mu\nu})(m_f^2 - K_{\parallel} \cdot P_{\parallel})]}{(K^2 - m_f^2)^2(P^2 - m_f^2)^2}, \quad (\text{B2})$$

$$\Pi_{(2,0)}^{\mu\nu}(Q) = -\sum_f 4ig^2(q_f B)^2 \int \frac{d^4K}{(2\pi)^4} \left[\frac{M^{\mu\nu}}{(K^2 - m_f^2)^4(P^2 - m_f^2)^2} \right], \quad (\text{B3})$$

where

$$\begin{aligned} M^{\mu\nu} &= K_{\perp}^2 [P^{\mu}K_{\parallel}^{\nu} + K_{\parallel}^{\mu}P^{\nu} - g^{\mu\nu}(K_{\parallel} \cdot P - m_f^2)] \\ &\quad + (m_f^2 - K_{\parallel}^2) [P^{\mu}K_{\perp}^{\nu} + K_{\perp}^{\mu}P^{\nu} - g^{\mu\nu}(K_{\perp} \cdot P)]. \end{aligned}$$

The complete gluon self-energy is expressed as

$$\Pi^{\mu\nu}(Q) = \Pi_{\text{YM}}^{\mu\nu}(Q) + \Pi_f^{\mu\nu}(Q),$$

where $\Pi_{\text{YM}}^{\mu\nu}$ refers to the Yang-Mills contribution to the gluon self-energy coming from the ghost and gluon loops, which is unaffected by the magnetic field. It is given by

$$\Pi_{\text{YM}}^{\mu\nu}(Q) = -\frac{N_c g^2 T^2}{3} \int \frac{d\Omega}{2\pi} \left(\frac{q_0 \hat{K}^{\mu} \hat{K}^{\nu}}{\hat{K} \cdot Q} - g^{\mu 0} g^{\nu 0} \right).$$

Using the properties of the tensors Δ_i , the form factors can be expressed as

$$\begin{aligned} b(Q) &= \Delta_1^{\mu\nu}(Q)\Pi_{\mu\nu}(Q) = \Delta_1^{\mu\nu}(\Pi_{\mu\nu}^{\text{YM}} + \Pi_{\mu\nu}^f) \\ &= b_{\text{YM}}(Q) + b_{0f}(Q) + b_{2f}(Q), \end{aligned} \quad (\text{B4})$$

$$\begin{aligned} c(Q) &= \Delta_2^{\mu\nu}(Q)\Pi_{\mu\nu}(Q) = \Delta_2^{\mu\nu}(\Pi_{\mu\nu}^{\text{YM}} + \Pi_{\mu\nu}^f) \\ &= c_{\text{YM}}(Q) + c_{0f}(Q) + c_{2f}(Q), \end{aligned} \quad (\text{B5})$$

$$\begin{aligned} d(Q) &= \Delta_3^{\mu\nu}(Q)\Pi_{\mu\nu}(Q) = \Delta_3^{\mu\nu}(\Pi_{\mu\nu}^{\text{YM}} + \Pi_{\mu\nu}^f) \\ &= d_{\text{YM}}(Q) + d_{0f}(Q) + d_{2f}(Q), \end{aligned} \quad (\text{B6})$$

$$\begin{aligned} a(Q) &= \frac{1}{2} \Delta_4^{\mu\nu}(Q)\Pi_{\mu\nu}(Q) = \frac{1}{2} \Delta_4^{\mu\nu}(\Pi_{\mu\nu}^{\text{YM}} + \Pi_{\mu\nu}^f) \\ &= a_{\text{YM}}(Q) + a_{0f}(Q) + a_{2f}(Q). \end{aligned} \quad (\text{B7})$$

In terms of powers of qB , the form factors can be expressed as

$$\begin{aligned} F(Q) &= F_0(Q) + F_2(Q) = [F_{\text{YM}}(Q) + F_{0f}(Q)] + F_{2f}(Q), \\ F &\equiv b, c, d, a. \end{aligned} \quad (\text{B8})$$

1. $\mathcal{O}(qB)^0$ terms of form factors

Using Eqs. (A11)–(A14) and (A18), we can write

$$\Delta_1^{00} = \bar{u}^2, \quad \Delta_2^{00} = \Delta_3^{00} = \Delta_4^{00} = 0, \quad \Pi^{00} = b\bar{u}^2.$$

Thus,

$$b_0(Q) = \frac{1}{\bar{u}^2} [\Pi_{00}^{\text{YM}}(Q) + \Pi_{00}^{(0,0)}(Q)]. \quad (\text{B9})$$

In the HTL approximation ($K \sim T$, $Q \sim gT$),

$$\begin{aligned} \Pi_{00}^{(0,0)}(Q) &= \frac{N_f g^2 T^2}{6} \left(1 - \frac{q_0}{2q} \log \frac{q_0 + q}{q_0 - q} \right), \\ \Pi_{00}^{\text{YM}} &= \frac{N_c g^2 T^2}{3} \left(1 - \frac{q_0}{2q} \log \frac{q_0 + q}{q_0 - q} \right). \end{aligned} \quad (\text{B10})$$

Thus,

$$b_0(Q) = \frac{m_D^2}{\bar{u}^2} \left(1 - \frac{q_0}{2q} \log \frac{q_0 + q}{q_0 - q} \right), \quad (\text{B11})$$

where $m_D^2 = (\Pi_{00}^{(0,0)} + \Pi_{00}^{\text{YM}})|_{p_0=0} = \frac{g^2 T^2}{3} (N_c + \frac{N_f}{2})$ is the QCD Debye screening mass in the absence of a magnetic field.

An alternate way of evaluating the form factors is to calculate the self-energy diagrammatically. As an example, the quark loop contribution to c_0 will be evaluated this way:

$$c_0^f(Q) = \left(g_{\perp}^{\mu\nu} - \frac{Q_{\perp}^{\mu} Q_{\perp}^{\nu}}{Q_{\perp}^2} \right) \Pi_{\mu\nu}^{(0,0)} = T_1 - T_2, \quad (\text{B12})$$

where

$$T_1 = g_{\perp}^{\mu\nu} \Pi_{\mu\nu}^{(0,0)}, \quad T_2 = \frac{Q_{\perp}^{\mu} Q_{\perp}^{\nu}}{Q_{\perp}^2} \Pi_{\mu\nu}^{(0,0)}.$$

Using the expression of $\Pi_{\mu\nu}^{(0,0)}$ from Eq. (B1) under the HTL approximation, we get

$$T_1 = -\sum_f 4g^2 (I_1 - I_2), \quad (\text{B13})$$

where

$$I_1 = \int \frac{d^3 k}{(2\pi)^3} T \sum_n \frac{K_{\perp}^2}{(K^2 - m_f^2)(P^2 - m_f^2)}, \quad (\text{B14})$$

$$I_2 = \int \frac{d^3 k}{(2\pi)^3} T \sum_n \frac{K^2}{(K^2 - m_f^2)(P^2 - m_f^2)}. \quad (\text{B15})$$

I_2 is a well-known integral which under the HTL approximation and in the limit of $m_f \rightarrow 0$ is $T^2/24$. The I_1 integral after summing over Matsubara frequencies simplifies to

$$\begin{aligned} I_1 &= -\frac{1}{2} \int \frac{d^3 k}{(2\pi)^3} \left[\frac{n_F(E_1)}{E_1} - \left(1 - \frac{q_0}{q_0 - q \cos \theta} \right) \frac{dn_F(E_1)}{dk} \right] \\ &\quad \times (\cos^2 \theta - 1). \end{aligned} \quad (\text{B16})$$

Here, $E_1 \approx k$ is the energy of the fermion propagator having 4-momentum K , θ is the polar angle made by \mathbf{k} , and n_F is the Fermi-Dirac distribution. First term in Eq. (B16) evaluates to $T^2/72$. The second term can be expanded as

$$\begin{aligned} &\frac{1}{8\pi^2} \int dk d(\cos \theta) k^2 \frac{dn_F(k)}{dk} \\ &\quad \times \left[\cos^2 \theta - 1 - \frac{q_0 \cos^2 \theta}{q_0 - q \cos \theta} + \frac{q_0}{q_0 - q \cos \theta} \right]. \end{aligned}$$

This evaluates term by term to

$$-T^2/72 + T^2/24 - \frac{q_0 T^2}{48q} \left[2 \frac{q_0}{q} + \frac{q_0^2}{q^2} \log \frac{q_0 + q}{q_0 - q} - \log \frac{q_0 + q}{q_0 - q} \right].$$

Thus,

$$I_1 - I_2 = -\frac{T^2}{48q^2} \left[2q_0^2 - (q_0^2 - q^2) \frac{q_0}{q} \log \frac{q_0 + q}{q_0 - q} \right]. \quad (\text{B17})$$

Similarly, it can be shown that

$$T_2 = -\sum_f 2g^2 (-I_1 + I_2 + I_3), \quad (\text{B18})$$

where

$$I_3(Q) = \int \frac{d^3 k}{(2\pi)^3} T \sum_n \frac{2k_1 k_2}{(K^2 - m_f^2)(P^2 - m_f^2)} = 0.$$

Thus,

$$\begin{aligned} c_0^f(Q) &= T_1 + T_2 = -\sum_f 2g^2 [I_1 - I - 2] \\ &= \frac{N_f g^2 T^2}{6} \frac{1}{2q^2} \left[q_0^2 - (q_0^2 - q^2) \frac{q_0}{2q} \log \frac{q_0 + q}{q_0 - q} \right]. \end{aligned} \quad (\text{B19})$$

The Yang-Mills contribution is given by

$$\frac{N_c g^2 T^2}{3} \frac{1}{2q^2} \left[q_0^2 - (q_0^2 - q^2) \frac{q_0}{2q} \log \frac{q_0 + q}{q_0 - q} \right].$$

Hence, finally,

$$c_0(q_0, q) = \frac{m_d^2}{2q^2} \left[q_0^2 - (q_0^2 - q^2) \frac{q_0}{2q} \log \frac{q_0 + q}{q_0 - q} \right]. \quad (\text{B20})$$

Next, we have

$$d_0(q_0, q) = \frac{\bar{n}^\mu \bar{n}^\nu}{\bar{n}^2} (\Pi_{\mu\nu}^{\text{YM}} + \Pi_{\mu\nu}^{(0,0)}). \quad (\text{B21})$$

It turns out that

$$d_0(q_0, q) = c_0(q_0, q) = \frac{m_d^2}{2q^2} \left[q_0^2 - (q_0^2 - q^2) \frac{q_0}{2q} \log \frac{q_0 + q}{q_0 - q} \right]. \quad (\text{B22})$$

The form factor a_0 is given by

$$\begin{aligned} a_0(q_0, q) &= \frac{1}{2} \Delta_4^{\mu\nu} (\Pi_{\mu\nu}^{\text{YM}} + \Pi_{\mu\nu}^{(0,0)}) \\ &= \frac{1}{2\sqrt{\bar{u}^2} \sqrt{\bar{n}^2}} \left[-2 \frac{\bar{u} \cdot n}{\bar{u}^2} [\Pi_{00}^{\text{YM}} + \Pi_{00}^{(0,0)}] \right. \\ &\quad \left. + 2[\Pi_{03}^{\text{YM}} + \Pi_{03}^{(0,0)}] \right] \\ &= 0. \end{aligned} \quad (\text{B23})$$

2. $\mathcal{O}(qB)^2$ terms of form factors

$$b_2(q_0, q) = \frac{u^\mu u^\nu}{\bar{u}^2} [\Pi_{\mu\nu}^{(1,1)} + 2\Pi_{\mu\nu}^{(2,0)}]. \quad (\text{B24})$$

Using Eqs. (B2) and (B3) in the above equation, we get

$$b_2(q_0, q) = -\sum_f \frac{2g^2(q_f B)^2}{\bar{u}^2} \int \frac{d^3k}{(2\pi)^3} T \sum_n \left\{ \frac{K^2 + k^2(1 + \cos^2\theta) + m_f^2}{(K^2 - m_f^2)^2(P^2 - m_f^2)^2} + \frac{8(k^4 + k^2 K^2)(1 - \cos^2\theta)}{(K^2 - m_f^2)^4(P^2 - m_f^2)} \right\}.$$

We make use of the HTL simplifications mentioned in Appendix C in [84] to further simplify b_2 to obtain

$$b_2 = -\sum_f \frac{2g^2(q_f B)^2}{\bar{u}^2} \int \frac{d^3k}{(2\pi)^3} T \sum_n \left\{ \frac{1}{(K^2 - m_f^2)^2(P^2 - m_f^2)} + \frac{(-7 + 9c^2)k^2 + 2m_f^2}{(K^2 - m_f^2)^3(P^2 - m_f^2)} - \frac{8(1 - c^2)(k^4 + m_f^2 k^2)}{(K^2 - m_f^2)^4(P^2 - m_f^2)} \right\},$$

where $c = \cos\theta$. Next, we perform the frequency sum using

$$\begin{aligned} T \sum_n \frac{1}{(\omega_n^2 + E_k^2)[(\omega_n - \omega)^2 + E_{k-q}^2]} &= \frac{[1 - n_F(E_k) - n_F(E_{k-q})]}{4E_k E_{k-q}} \left\{ \frac{1}{i\omega + E_k + E_{k-q}} - \frac{1}{i\omega - E_k - E_{k-q}} \right\} \\ &\quad + \frac{[n_F(E_k) - n_F(E_{k-q})]}{4E_k E_{k-q}} \left\{ \frac{1}{i\omega + E_k - E_{k-q}} - \frac{1}{i\omega - E_k + E_{k-q}} \right\}, \end{aligned}$$

where $E_k = \sqrt{k^2 + m_f^2}$ and $E_{k-q} = \sqrt{(k-q)^2 + m_f^2}$. We write the expression in terms of mass derivatives to finally obtain

$$\begin{aligned} b_2(q_0, q) &= \sum_f \frac{2g^2 q_f^2 B^2}{\bar{u}^2} \left\{ \left(\frac{\partial^2}{\partial^2(m_f^2)} + \frac{5}{6} m_f^2 \frac{\partial^3}{\partial^3(m_f^2)} \right) \int \frac{d^3k}{(2\pi)^3} \frac{n_F(E_k)}{E_k} \left(\frac{q_0}{q_0 - q \cos\theta} - 1 \right) \right. \\ &\quad + \left(\frac{\partial}{\partial(m_f^2)} + \frac{5}{6} m_f^2 \frac{\partial^2}{\partial^2(m_f^2)} \right) \int \frac{d^3k}{(2\pi)^3} \frac{n_F(E_k)}{2E_k^3} \left(\frac{q_0}{q_0 - q \cos\theta} \right) \\ &\quad - \left(\frac{\partial^2}{\partial^2(m_f^2)} + \frac{m_f^2}{2} \frac{\partial^3}{\partial^3(m_f^2)} \right) \int \frac{d^3k}{(2\pi)^3} \frac{n_F(E_k)}{E_k} \cos^2\theta \left(\frac{q_0}{q_0 - q \cos\theta} - 1 \right) \\ &\quad \left. - \left(\frac{\partial}{\partial(m_f^2)} + \frac{m_f^2}{2} \frac{\partial^2}{\partial^2(m_f^2)} \right) \int \frac{d^3k}{(2\pi)^3} \frac{n_F(E_k)}{2E_k^3} \cos^2\theta \left(\frac{q_0}{q_0 - q \cos\theta} \right) \right\}. \end{aligned}$$

After simplification, we finally obtain

$$b_2 = \frac{\delta m_D^2}{\bar{u}^2} + \sum_f \frac{g^2(q_f B)^2}{\bar{u}^2 \pi^2} \times \left[\left(g_k + \frac{\pi m_f - 4T}{32m_f^2 T} \right) (A_0 - A_2) + \left(f_k + \frac{8T - \pi m_f}{128m_f^2 T} \right) \left(\frac{5A_0}{3} - A_2 \right) \right]. \quad (\text{B25})$$

Here, δm_D^2 is the correction to the Debye mass due to weak magnetic field given by

$$\begin{aligned}\delta m_D^2 &= [\Pi_{\mu\nu}^{(1,1)} + 2\Pi_{\mu\nu}^{(2,0)}]_{q_0=0, q \rightarrow 0} = \sum_f \frac{g^2}{12\pi^2 T^2} (q_f B)^2 \sum_{l=1}^{\infty} (-1)^{l+1} l^2 K_0 \left(\frac{m_f l}{T} \right), \\ f_k &= - \sum_{l=1}^{\infty} (-1)^{l+1} \frac{l^2}{16T^2} K_2 \left(\frac{m_f l}{T} \right), \\ g_k &= \sum_{l=1}^{\infty} (-1)^{l+1} \frac{l}{4m_f T} K_1 \left(\frac{m_f l}{T} \right), \\ A_0 &= \int \frac{d\Omega}{4\pi} \frac{q_0 c^0}{Q \cdot \hat{K}} = \frac{q_0}{2q} \log \left(\frac{q_0 + q}{q_0 - q} \right), \\ A_2 &= \int \frac{d\Omega}{4\pi} \frac{q_0 c^2}{Q \cdot \hat{K}} = \frac{q_0^2}{2q^2} \left(1 - \frac{3q_3^2}{q^2} \right) \left(1 - \frac{q_0}{2q} \log \frac{q_0 + q}{q_0 - q} \right) + \frac{1}{2} \left(1 - \frac{q_3^2}{q^2} \right) \frac{q_0}{2q} \log \frac{q_0 + q}{q_0 - q}.\end{aligned}$$

K_0 , K_1 , and K_2 are the modified Bessel functions of the second kind. Similarly, the form factor c_2 is given by

$$c_2(q_0, q) = \left(g_{\perp}^{\mu\nu} - \frac{Q_{\perp}^{\mu} Q_{\perp}^{\nu}}{Q_{\perp}^2} \right) [\Pi_{\mu\nu}^{(1,1)} + 2\Pi_{\mu\nu}^{(2,0)}]. \quad (\text{B26})$$

Using Eqs. (B2) and (B3), we get

$$\begin{aligned}c_2(q_0, q) &= - \sum_f \frac{g^2 (q_f B)^2}{2} \int \frac{d^3 k}{(2\pi)^3} T \sum_n \left[\frac{4k_0^2 - 4k_3^2 - 4m_f^2}{(K^2 - m_f^2)^2 (P^2 - m_f^2)^2} + \frac{4(4k_3^2 - 4k_0^2 + 4m_f^2)}{(K^2 - m_f^2)^3 (P^2 - m_f^2)} \right. \\ &\quad \left. - \frac{4(k_0^2 - k_3^2 - m_f^2)(8k_{\perp}^2 - 4K^2 + 4m_f^2 + 8(\mathbf{k} \cdot \mathbf{q})_{\perp}^2 / q_{\perp}^2)}{(K^2 - m_f^2)^4 (P^2 - m_f^2)} \right].\end{aligned}$$

Using HTL approximations to simplify as earlier, we write c_2 in terms of mass derivatives as earlier:

$$\begin{aligned}c_2 &= - \sum_f 2g^2 (q_f B)^2 \int \frac{d^3 k}{(2\pi)^3} T \sum_n \left[\frac{1}{2} + \frac{1}{4} (1 - \cos^2 \theta) \cos^2 \phi + \frac{7}{4} \sin^2 \theta (1 + \cos^2 \phi) - \frac{5}{4} \sin^4 \theta (1 + \cos^2 \phi) \right] \\ &\quad \times \frac{\partial}{\partial (m_f^2)} \frac{1}{(K^2 - m_f^2)(P^2 - m_f^2)}.\end{aligned}$$

After performing the frequency sum followed by the integral, we finally obtain

$$\begin{aligned}c_2(q_0, q) &= - \sum_f \frac{4g^2 (q_f B)^2}{3\pi^2} g_k + \frac{g^2 (q_f B)^2}{2\pi^2} \left(g_k + \frac{\pi m_f - 4T}{32m_f^2 T} \right) \times \left[-\frac{7}{3} \frac{q_0^2}{q_{\perp}^2} + \left(2 + \frac{3}{2} \frac{q_0^2}{q_{\perp}^2} \right) A_0 \right. \\ &\quad \left. + \left(\frac{3}{2} + \frac{5}{2} \frac{q_0^2}{q_{\perp}^2} + \frac{3}{2} \frac{q_3^2}{q_{\perp}^2} \right) A_2 - \frac{3q_0 q_3}{q_{\perp}^2} A_1 - \frac{5}{2} \left(1 - \frac{q_3^2}{q_{\perp}^2} \right) A_4 - \frac{5q_0 q_3}{q_{\perp}^2} A_3 \right]. \quad (\text{B27})\end{aligned}$$

The remaining A integrals are

$$\begin{aligned}A_1 &= - \frac{q_0 q_3}{q^2} \left[1 - \frac{q_0}{2q} \log \left(\frac{q_0 + q}{q_0 - q} \right) \right], \\ A_3 &= \frac{q_0 q_3}{2q} \left(1 - \frac{5q_3^2}{3q^2} \right) - \frac{3q_0 q_3}{2q} \left(1 - \frac{q_0^2}{q^2} - \frac{q_3^2}{q^2} + \frac{5q_0^2 q_3^2}{3q^2 q^2} \right) \times \left(1 - \frac{q_0}{2q} \log \frac{q_0 + q}{q_0 - q} \right), \\ A_4 &= \frac{3}{8} \left(1 - \frac{q_3^2}{q^2} \right)^2 - \frac{q_0^2}{8q^2} \left(1 - \frac{5q_3^2}{q^2} \right)^2 + \frac{5q_0^2 q_3^4}{3q^2 q^4} - \frac{3}{8} \left\{ \left(1 - \frac{q_0^2}{q^2} \right)^2 - \frac{2q_3^2}{q^2} \left(1 - \frac{3q_0^2}{q^2} \right)^2 \right. \\ &\quad \left. + \frac{q_3^4}{q^4} \left(1 - \frac{5q_0^2}{q^2} \right)^2 + \frac{8q_0^4 q_3^2}{q^4 q^2} \left(1 - \frac{5q_3^2}{3q^2} \right) \right\} \times \left(1 - \frac{q_0}{2q} \log \frac{q_0 + q}{q_0 - q} \right).\end{aligned}$$

It should be noted that the imaginary parts of the form factors come from the imaginary parts of the A_i 's. We write down the final expressions. The detailed derivation can be found in [84]:

$$d_2(q_0, q) = \frac{\bar{n}^\mu \bar{n}^\nu}{\bar{n}^2} [\Pi_{\mu\nu}^{(1,1)} + 2\Pi_{\mu\nu}^{(2,0)}] = F_1 + F_2, \quad (\text{B28})$$

where

$$F_1 = -\sum_f \frac{g^2 (q_f B)^2 q^2}{\pi^2 q_\perp^2} \times \left[g_k \left\{ \frac{q_0^2 q_3^2}{3q^4} + \frac{A_0}{4} - \left(\frac{3}{2} + \frac{q_0^2 q_3^2}{q^4} \right) A_2 + \frac{5}{4} A_4 \right\} + \left(\frac{\pi}{32m_f T} - \frac{1}{8m_f^2} \right) \left\{ \frac{A_0}{4} - \left(\frac{3}{2} + \frac{q_0^2 q_3^2}{p^4} \right) A_2 + \frac{5}{4} A_4 \right\} \right. \\ \left. - f_k \frac{q_0^2 q_3^2}{q^4} \left(\frac{14}{3} - 5A_0 + A_2 \right) + \frac{q_0^2 q_3^2}{q^4} \frac{8T - \pi m_f}{128Tm_f^2} (5A_0 - A_2) \right], \\ F_2 = -\sum_f \frac{g^2 (q_f B)^2 q^0 q^3}{6\pi^2 m_f T} \frac{1}{q_\perp^2} \frac{1}{1 + \cosh \frac{m_f}{T}} \times \left(\frac{3A_1}{2} - A_3 \right).$$

Finally,

$$a_2(q_0, q) = \frac{1}{2} \left(\frac{\bar{u}^\mu \bar{n}^\nu + \bar{u}^\nu \bar{n}^\mu}{\sqrt{\bar{u}^2} \sqrt{\bar{n}^2}} \right) [\Pi_{\mu\nu}^{(1,1)} + 2\Pi_{\mu\nu}^{(2,0)}] = G_1 + G_2, \quad (\text{B29}) \\ G_1 = \sum_f \frac{4g^2 (q_f B)^2}{2\pi^2 \sqrt{\bar{u}^2} \sqrt{\bar{n}^2}} \times \left[\frac{q_0 q_3}{q^2} \left\{ \left(\frac{2}{3} - A_0 + A_2 \right) g_k + \left(\frac{4}{3} - \frac{5A_0}{3} + A_2 \right) f_k \right\} \right. \\ \left. + \left\{ (-A_0 + A_2) \frac{\pi m_f - 4T}{32Tm_f^2} - \frac{1}{6} (5A_0 - 3A_2) \frac{8T - \pi m_f}{64Tm_f^2} \right\} \right], \\ G_2 = \sum_f \frac{g^2 (q_f B)^2}{\sqrt{\bar{u}^2} \sqrt{\bar{n}^2} 6\pi^2 m_f T \left(1 + \cosh \frac{m_f}{T} \right)} \times (-5A_1 + 4A_3).$$

APPENDIX C: CALCULATION OF SPECTRAL FUNCTIONS ρ_i

The cut parts of the spectral functions are evaluated from the discontinuity in the pieces of the gluon propagators, which, in turn, is given by their imaginary parts analytically continued to real values of energy:

$$\rho_1(\omega, q) = -\frac{1}{\pi} \text{Im}(\chi_1|_{q_0=\omega+i\epsilon}) \\ = -\frac{1}{\pi} \text{Im} \left(\frac{(Q^2 - d)}{(Q^2 - b)(Q^2 - d) - a^2} \Big|_{q_0=\omega+i\epsilon} \right) \\ = -\frac{1}{\pi D} [\text{Im}_b(\text{Im}_d^2 + \text{Re}_d^2 + Q^4 - 2Q^2 \text{Re}_d) + 2\text{Im}_a \text{Re}_a(Q^2 - \text{Re}_d) + \text{Im}_d(\text{Re}_d^2 - \text{Im}_d^2)].$$

Here, Im and Re, respectively, depict the imaginary and real parts of the form factors.

$$\rho_2(\omega, q) = -\frac{1}{\pi} \text{Im}(\chi_2|_{q_0=\omega+i\epsilon}) = -\frac{1}{\pi} \text{Im} \left(\frac{1}{(Q^2 - c)} \Big|_{q_0=\omega+i\epsilon} \right) = -\frac{1}{\pi} \left[\frac{\text{Im}_c}{\text{Im}_c^2 - (Q^2 - \text{Re}_c)^2} \right], \\ \rho_3(\omega, q) = -\frac{1}{\pi} \text{Im}(\chi_3|_{q_0=\omega+i\epsilon}) \\ = -\frac{1}{\pi} \text{Im} \left(\frac{(Q^2 - b)}{(Q^2 - b)(Q^2 - d) - a^2} \Big|_{q_0=\omega+i\epsilon} \right) \\ = -\frac{1}{\pi D} [\text{Im}_d(\text{Im}_b^2 + \text{Re}_b^2 + Q^4 - 2Q^2 \text{Re}_b) + 2\text{Im}_a \text{Re}_a(Q^2 - \text{Re}_b) + \text{Im}_b(\text{Re}_d^2 - \text{Im}_d^2)],$$

$$\begin{aligned}
\rho_4(\omega, q) &= -\frac{1}{\pi} \text{Im}(\chi_4|_{q_0=\omega+ic}) \\
&= -\frac{1}{\pi} \text{Im}\left(\frac{a}{(Q^2-b)(Q^2-d)-a^2}\Big|_{q_0=\omega+ic}\right) \\
&= -\frac{1}{\pi D} [\text{Im}_a\{-\text{Im}_b\text{Im}_d + \text{Re}_b\text{Re}_d + \text{Re}_a^2 + \text{Im}_a^2 + Q^4 - Q^2(\text{Re}_b + \text{Re}_d)\} \\
&\quad + \text{Re}_a(Q^2(\text{Im}_b + \text{Im}_d)\text{Im}_d\text{Re}_b - \text{Im}_b\text{Re}_d)].
\end{aligned}$$

Here, the denominator D is expressed as

$$D = [(-\text{Im}_b Q^2 - \text{Im}_d Q^2 + \text{Im}_d \text{Re}_b + \text{Im}_b \text{Re}_d - 2\text{Im}_a \text{Re}_a)^2 + (-\text{Im}_b \text{Im}_d + \text{Im}_a^2 + (Q^2 - \text{Re}_b)(Q^2 - \text{Re}_d) - \text{Re}_a^2)^2].$$

-
- [1] I. Arsene *et al.* (BRAHMS Collaboration), *Nucl. Phys.* **A757**, 1 (2005).
- [2] J. Adams *et al.* (STAR Collaboration), *Nucl. Phys.* **A757**, 102 (2005).
- [3] P. F. Kolb and U. W. Heinz, *Quark-Gluon Plasma* (World Scientific, Singapore, 2004), Vol. 3, p. 63.
- [4] E. V. Shuryak, *Nucl. Phys.* **A750**, 64 (2005).
- [5] P. Huovinen and P. V. Ruuskanen, *Annu. Rev. Nucl. Part. Sci.* **56**, 163 (2006).
- [6] T. Hirano, *J. Phys. G* **36**, 064031 (2009).
- [7] P. K. Kovtun, D. T. Son, and A. O. Starinets, *Phys. Rev. Lett.* **94**, 111601 (2005).
- [8] A. D. Frawley, T. Ullrich, and R. Vogt, *Phys. Rep.* **462**, 125 (2008).
- [9] P. Lévai, B. Müller, and X. N. Wang, *Phys. Rev. C* **51**, 3326 (1995).
- [10] S. K. Das, S. Plumari, S. Chatterjee, J. Alam, F. Scardina, and V. Greco, *Phys. Lett. B* **768**, 134955 (2019).
- [11] U. Heinz, *AIP Conf. Proc.* **739**, 163 (2004).
- [12] M. He, H. V. Hees, and R. Rapp, *Prog. Part. Nucl. Phys.* **130**, 104020 (2023).
- [13] R. Rapp and H. V. Hees, *Quark Gluon Plasma* (World Scientific, Singapore, 2010), Vol. 4, p. 111.
- [14] K. Tuchin, *Adv. High Energy Phys.* **2013**, 490495 (2013).
- [15] K. Tuchin, *Phys. Rev. C* **82**, 034904 (2010).
- [16] K. Tuchin, *Phys. Rev. C* **83**, 017901 (2011).
- [17] R. Marty, E. Bratkovskaya, W. Cassing, J. Aichelin, and H. Berrehrh, *Phys. Rev. C* **88**, 045204 (2013).
- [18] H.-T. Ding, A. Francis, O. Kaczmarek, F. Karsch, E. Laermann, and W. Soeldner, *Phys. Rev. D* **83**, 034504 (2011).
- [19] A. Amato, G. Aarts, C. Allton, P. Giudice, S. Hands, and J.-I. Skullerud, *Phys. Rev. Lett.* **111**, 172001 (2013).
- [20] G. Aarts, C. Allton, J. Foley, S. Hands, and S. Kim, *Phys. Rev. Lett.* **99**, 022002 (2007).
- [21] A. Puglisi, S. Plumari, and V. Greco, *Phys. Rev. D* **90**, 114009 (2014).
- [22] M. Greif, I. Bouras, C. Greiner, and Z. Xu, *Phys. Rev. D* **90**, 094014 (2014).
- [23] K. Hattori, X. G. Huang, D. H. Rischke, and D. Satow, *Phys. Rev. D* **96**, 094009 (2017).
- [24] S. Gupta, *Phys. Lett. B* **597**, 57 (2004); *Phys. Rev. C* **88**, 024911 (2013); **93**, 014905 (2016); *Nucl. Phys.* **A929**, 184 (2014).
- [25] D. E. Kharzeev, L. D. McLerran, and H. J. Warringa, *Nucl. Phys.* **A803**, 227 (2008).
- [26] D. E. Kharzeev and H. U. Yee, *Phys. Rev. D* **83**, 085007 (2011).
- [27] G. M. Newman, *J. High Energy Phys.* **01** (2006) 158.
- [28] Y. Burnier, D. E. Kharzeev, J. Liao, and H. U. Yee, *Phys. Rev. Lett.* **107**, 052303 (2011).
- [29] E. V. Gorbar, V. A. Miransky, and I. A. Shovkovy, *Phys. Rev. D* **83**, 085003 (2011).
- [30] J. Alexandre, K. Farakos, and G. Koutsoumbas, *Phys. Rev. D* **63**, 065015 (2001).
- [31] V. P. Gusynin and I. A. Shovkovy, *Phys. Rev. D* **56**, 5251 (1997).
- [32] D. S. Lee, C. N. Leung, and Y. J. Ng, *Phys. Rev. D* **55**, 6504 (1997).
- [33] G. S. Bali, F. Bruckmann, G. Endrodi, Z. Fodor, S. D. Katz, S. Krieg, A. Schafer, and K. K. Szabo, *J. High Energy Phys.* **02** (2012) 044.
- [34] R. L. S. Farias, K. P. Gomes, G. I. Krein, and M. B. Pinto, *Phys. Rev. C* **90**, 025203 (2014).
- [35] R. L. S. Farias, V. S. Timoteo, S. S. Avancini, M. B. Pinto, and G. Krein, *Eur. Phys. J. A* **53**, 101 (2017).
- [36] N. Mueller and J. M. Pawłowski, *Phys. Rev. D* **91**, 116010 (2015).
- [37] A. Ayala, M. Loewe, A. Z. Mizher, and R. Zamora, *Phys. Rev. D* **90**, 036001 (2014).
- [38] A. Ayala, M. Loewe, and R. Zamora, *Phys. Rev. D* **91**, 016002 (2015).
- [39] A. Ayala, C. A. Dominguez, L. A. Hernandez, M. Loewe, and R. Zamora, *Phys. Lett. B* **759**, 99 (2016).
- [40] G. Aarts, C. Allton, A. Amato, P. Giudice, S. Hands, and J.-I. Skullerud, *J. High Energy Phys.* **02** (2015) 186.
- [41] H.-T. Ding, O. Kaczmarek, and F. Meyer, *Phys. Rev. D* **94**, 034504 (2016).
- [42] S. Rath and B. K. Patra, *Phys. Rev. D* **100**, 016009 (2019).
- [43] S. A. Khan and B. K. Patra, *Phys. Rev. D* **104**, 054024 (2021).

- [44] S. Li and H. Yee, *Phys. Rev. D* **97**, 056024 (2018).
- [45] P. Panday and B. K. Patra, *Int. J. Mod. Phys.* **33**, 2450010 (2024).
- [46] M. Kurian, *Phys. Rev. D* **103**, 054024 (2021).
- [47] S. A. Khan and B. K. Patra, *Phys. Rev. D* **107**, 074034 (2023).
- [48] D. Dey and B. K. Patra, *Phys. Rev. D* **104**, 076021 (2021).
- [49] M. Hasan and B. K. Patra, *Phys. Rev. D* **102**, 036020 (2020).
- [50] K. Fukushima, K. Hattori, Ho-Ung Yee, and Y. Yin, *Phys. Rev. D* **93**, 074028 (2016).
- [51] B. Singh, S. Mazumder, and H. Mishra, *J. High Energy Phys.* **05** (2020) 068.
- [52] A. Bandyopadhyay, J. Liao, and H. Xing, *Phys. Rev. D* **105**, 114049 (2022).
- [53] M. Y. Jamal, J. Prakash, I. Nilima, and A. Bandyopadhyay, *J. Phys. G* **51**, 045104 (2024).
- [54] M. H. Thoma and M. Gyulassy, *Nucl. Phys.* **B351**, 491 (1991).
- [55] E. Braaten and M. H. Thoma, *Phys. Rev. D* **44**, 1298 (1991).
- [56] G. D. Moore and D. Teaney, *Phys. Rev. C* **71**, 064904 (2005).
- [57] M. Monteno, W. M. Alberico, A. Beraudo, A. De Pace, A. Molinari, M. Nardi, and F. Prino, *J. Phys. G* **38**, 124144 (2011).
- [58] M. He, R. J. Fries, and R. Rapp, *Phys. Lett. B* **735**, 445 (2014).
- [59] A. Beraudo, A. De Pace, M. Monteno, M. Nardi, and F. Prino, *Eur. Phys. J. C* **75**, 121 (2015).
- [60] S. K. Das, F. Scardina, S. Plumari, and V. Greco, *Phys. Lett. B* **747**, 260 (2015).
- [61] A. V. Sadofyev and Y. Yin, *Phys. Rev. D* **93**, 125026 (2016).
- [62] Y. Akamatsu, *Phys. Rev. C* **92**, 044911 (2015).
- [63] A. Andronic *et al.*, *Eur. Phys. J. C* **76**, 107 (2016).
- [64] M. Kurian, S. K. Das, and V. Chandra, *Phys. Rev. D* **100**, 074003 (2019).
- [65] B. Singh, M. Kurian, S. Mazumder, H. Mishra, V. Chandra, and S. K. Das, [arXiv:2004.11092](https://arxiv.org/abs/2004.11092).
- [66] D. Banerjee, S. Datta, and R. Gavai, *Phys. Rev. D* **85**, 014510 (2012).
- [67] A. Bouteffeux and M. Laine, *J. High Energy Phys.* **12** (2020) 150.
- [68] D. Banerjee, S. Datta, and M. Laine, *J. High Energy Phys.* **08** (2022) 128.
- [69] S. Caron-Huot, M. Laine, and G. D. Moore, *J. High Energy Phys.* **04** (2009) 053.
- [70] B. Singh, A. Abhishek, S. K. Das, and H. Mishra, *Phys. Rev. D* **100**, 114019 (2019).
- [71] S. Chatterjee and P. Bożek, *Phys. Lett. B* **798**, 134955 (2017).
- [72] Jun-Hong Liu, S. K. Das, V. Greco, and M. Ruggieri, *Phys. Rev. D* **103**, 034029 (2021).
- [73] S. Mrówczyński, *Eur. Phys. J. A* **54**, 43 (2018).
- [74] K. Rajagopal and A. V. Sadofyev, *J. High Energy Phys.* **10** (2015) 018.
- [75] J. Casalderrey-Solana and D. Teaney, *Phys. Rev. D* **74**, 085012 (2006).
- [76] S. Caron-Huot and G. D. Moore, *Phys. Rev. Lett.* **100**, 052301 (2008); *J. High Energy Phys.* **02** (2008) 081.
- [77] A. Kumar, M. Kurian, S. K. Das, and V. Chandra, *Phys. Rev. C* **105**, 054903 (2022).
- [78] J. Prakash, V. Chandra, and S. K. Das, *Phys. Rev. D* **108**, 096016 (2023).
- [79] S. Mazumder, V. Chandra, and S. K. Das, [arXiv:2211.06985](https://arxiv.org/abs/2211.06985).
- [80] H. A. Weldon, *Phys. Rev. D* **28**, 2007 (1983).
- [81] F. Reif, *Fundamentals of Statistical and Thermal Physics* (McGraw-Hill, New York, 1965).
- [82] L. D. Landau and E. M. Lifshitz, *Statistical Physics* (Addison-Wesley, Reading, MA, 1969).
- [83] M. H. Thoma, [arXiv:hep-ph/0010164](https://arxiv.org/abs/hep-ph/0010164).
- [84] B. Karmakar, A. Bandyopadhyay, N. Haque, and M. G. Mustafa, *Eur. Phys. J. C* **79**, 658 (2019).
- [85] R. D. Pisarski, *Nucl. Phys.* **B309**, 476 (1988).
- [86] R. D. Pisarski, *Nucl. Phys.* **A498**, 423 (1989).
- [87] A. Bazavov, N. Brambilla, X. Garcia i Tormo, P. Petreczky, J. Soto, and A. Vairo, *Phys. Rev. D* **86**, 114031 (2012).
- [88] K. Hattori, S. Li, D. Satow, and H.-U. Yee, *Phys. Rev. D* **95**, 076008 (2017).
- [89] A. Beraudo, A. De Pace, W. M. Alberico, and A. Molinari, *Nucl. Phys.* **A831**, 59 (2009).
- [90] B. Svetitsky, *Phys. Rev. D* **37**, 2484 (1988); *Phys. Rev. Lett.* **99**, 192301 (2007); *Nucl. Phys.* **B483**, 291 (1997); *Phys. Rev. Lett.* **103**, 142302 (2009); *Phys. Rev. D* **89**, 014002 (2014).